การเปลี่ยนแปลงรูปร่างแผ่นเปลือกโลกของประเทศไทย โดยใช้ข้อมูลการตรวจวัดจากระบบพิกัดตำแหน่ง
(จีพีเอส) และการวิเคราะห์ความเครียด

นางสาวสรัลธร บำรุงวงศ์

511540

CRUSTAL DEFORMATION IN THAILAND USING GLOBAL POSITIONING SYSTEM (GPS) DATA

AND STRAIN ANALYSIS

Miss Sarandhorn Bamrungwong

A Thesis Submitted in Partial Fulfillment of the Requirements

for the Degree of Master of Science Program in Earth Sciences

Department of Geology

Faculty of Science

Chulalongkorn University

Academic Year 2008

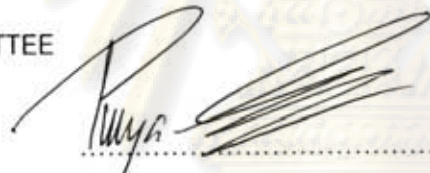Thesis Title CRUSTAL DEFORMATION IN THAILAND USING GLOBAL
POSITIONING SYSTEM (GPS) DATA AND STRAIN ANALYSIS

By Miss Sarandhorn Bamrungwong

Field of Study Earth Sciences

Thesis Principal Advisor Associate Professor Chalermchon Satirapod, Ph.D

Thesis Co-advisor Miss Boossarasiri Thana, M.Sc.

Accepted by the Faculty of Science, Chulalongkorn University in Partial Fulfillment of the Requirements for the Master's Degree

.... Dean of the Faculty of Science

(Professor Supot Hannongbua, Dr.rer.nat.)

THESIS COMMITTEE

.... Chairman

(Associate Professor Punya Charusiri, Ph.D.)

.... Thesis Principal Advisor

(Associate Professor Chalermchon Satirapod, Ph.D.)

.... Thesis Co-advisor

(Miss Boossarasiri Thana)

.... Member

(Assistant Professor Somchai Nakapadungrat, Ph.D.)

.... Member

(Assistant Professor Nopadon Muangnoicharoen, Ph.D.)

สรัลธร บำรุงวงศ์ : การเปลี่ยนแปลงรูปร่างแผ่นเปลือกโลกของประเทศไทย โดยใช้ข้อมูลการตรวจวัดจากระบบพิกัดตำแหน่ง (จีพีเอส) และการวิเคราะห์ความเครียด. (CRUSTAL DEFORMATION IN THAILAND USING GLOBAL POSITIONING SYSTEM (GPS) DATA AND STRAIN ANALYSIS) อ.ที่ปรึกษาวิทยานิพนธ์หลัก : รศ. ดร.เฉลิมชนม์ สถิระพจน์, อ.ที่ปรึกษาวิทยานิพนธ์ร่วม : นางสาว บุศราศิริ ธนะ, 64 หน้า.

วัตถุประสงค์ของงานวิจัยนี้ เพื่อศึกษาการเปลี่ยนแปลงรูปร่างแผ่นเปลือกโลกย่อยซุนดา โดยเฉพาะบริเวณประเทศไทย ในช่วงก่อนและหลังเกิดแผ่นดินไหวใหญ่สุมาตรา-อันดามัน เมื่อวันที่ 26 ธันวาคม พ.ศ. 2547 โดยใช้ข้อมูลข้อมูลการตรวจวัดจากระบบพิกัดตำแหน่ง (จีพีเอส) และการวิเคราะห์ความเครียด งานวิจัยนี้ได้ศึกษาข้อมูลการเคลื่อนตัวของประเทศไทยโดยรวบรวมข้อมูลจีพีเอสตั้งแต่ปี พ.ศ. 2537 – 2549 ที่ได้จากสถานีฐานในประเทศไทย 6 สถานีซึ่งตั้งอยู่ในจังหวัดต่างๆ ได้แก่ ภูเก็ต ชุมพร ชลบุรี อุทัยธานี ศรีสะเกษ และลำปาง และข้อมูลจีพีเอสของสถานีทางตอนเหนือของมาเลเซียอีก 1 สถานี

ตั้งแต่ปี พ.ศ. 2537 – 2547 ก่อนเกิดแผ่นดินไหวใหญ่เมื่อวันที่ 26 ธันวาคม พ.ศ.2547 พบว่าในตลอดระยะเวลา 10 ปีนั้น ประเทศไทยทั้งประเทศมีการเคลื่อนตัวในทางราบด้วยความเร็วไปทางทิศตะวันออก ในขนาดที่ใกล้เคียงกัน ซึ่งเฉลี่ยทั้งประเทศมีความเร็วประมาณ 33.2 ± 1.1 มิลลิเมตรต่อปี และเมื่อวิเคราะห์อัตราความเครียดทางราบพบว่ามีขนาดเล็กกว่า 0.03 ไมโครสเตรนต่อปี ซึ่งเป็นขนาดที่แทบจะไม่มีนัยสำคัญ แต่กระนั้นก็สามารถเห็นรูปแบบบางอย่างที่มีความสัมพันธ์กับการเคลื่อนตัวของรอยเลื่อนสะแกง หลังจากเกิดแผ่นดินไหวครั้งใหญ่นั้น ทำให้ทิศทางการเคลื่อนตัวในทางราบไปทางทิศตะวันตกเฉียงใต้ในขนาดที่แตกต่างกัน ทำให้ประเทศไทยเกิดอัตราความเครียดหลักแบบยืดออก ในทิศตะวันออกเฉียงเหนือ-ตะวันตกเฉียงใต้ ซึ่งมีความสอดคล้องกับการเคลื่อนตัวของร่องสุมาตรา นอกจากนี้หลังเกิดแผ่นดินไหวในแอสเมื่อวันที่ 28 มีนาคม พ.ศ.2548 มีรูปแบบของความเร็วและอัตราความเครียดของแผ่นดิน ก็มีความคล้ายคลึงกับการเกิดแผ่นดินไหวใหญ่ ดังนั้นจึงกล่าวได้ว่าแผ่นดินไหวในแอสเป็นแผ่นดินไหวต่อเนื่องจากแผ่นดินไหวใหญ่

ภาควิชา	ธรณีวิทยา	ลายมือชื่อนิสิต..
สาขาวิชา	โลกศาสตร์	ลายมือชื่อ อ.ที่ปรึกษาวิทยานิพนธ์หลัก....................
ปีการศึกษา	2551	ลายมือชื่อ อ.ที่ปรึกษาวิทยานิพนธ์ร่วม....................

487 26083 23   : MAJOR EARTH SCIENCES

KEY WORD: CRUSTAL DEFORMATION / STRAIN ANALYSIS / GPS

SARANDHORN BAMRUNGWONG : CRUSTAL DEFORMATION IN THAILAND USING GLOBAL POSITIONING SYSTEM (GPS) DATA AND STRAIN ANALYSIS. THESIS PRINCIPAL ADVISOR : ASSOC. PROF. CHALERMCHON SATIRAPOD, Ph.D., THESIS COADVISOR : MISS BOOSSARASIRI THANA, 64 pp.

The objective of this research is to study how Sudaland block, especially Thailand, deforms before and after the Sumatra-Andaman 2004 mega-earthquake by using GPS measurement and strain analysis. The studies used data, colleted between 1994 and 2006, from 6 regional GPS sites consisting of Phuket, Chumporn, Chonburi, Uthaithanee, Srisaket and Lampang in Thailand, and one GPS site from the northern part of Malaysia.

During 1994-2004 before the mega-earthquake on the December 26, 2004, it was found that Thailand as the whole area had moved horizontally nearly at the same rate to the east with the average rate of approximately 33.2 ± 1.1 millimeters per year. The horizontal strain rate was found to be less than 30 nanostrain per year, which was not significant. However, this horizontal strain rate showed the similarity in pattern as the movement of Sagaing fault. After the mega-earthquake, it caused the change of horizontal movement in the direction to southwest at the different rates. It was also found that Thailand has the principal strain rate tensors as the extension type in the direction of northeast – southwest. The strain rate tensors were agreed with the movement of Sumatran trench. In addition, the results revealed that the Nias earthquake produced the same velocities and strain rates pattern as the mega-earthquake. This implies that the Nias earthquake is an aftershock of the mega-earthquake.

Department : Geology	Student's signature :
Field of study : Earth Sciences	Principal Advisor's signature :
Academic year : 2008	Co-advisor's signature : B. Thana

ACKNOWLEDGEMENTS

This thesis is based on the M.Sc. program carried out under the guidance of my advisor Associate Professor Dr. Chalermchon Satirapod, Department of Survey Engineering, Faculty of Engineering, Chulalongkorn University and my co-advisor Miss Boossarasiri Thana, Department of Geology, Faculty of Science, Chulalongkorn University. Dr Chalermchon guided me with patience and enthusiasm for approaching my study logically, providing all knowledge of the field and completing thesis. Miss Boossarasiri also gave me precious suggestion throughout this thesis work. I am indebted to the Royal Thai Survey Department (RTSD) and Dr. Wim Simons of Delf University of Technology who provided me all the GPS Data. I have a deep gratitude towards Professor Dr. Manabu Hashimoto of Disaster Prevention Research Institue, Kyoto University and Professor Dr. Michio Hashizume for expanding my knowledge and a lot of ideas. My special thanks are due to Associate Professor Dr. Punya Charusiri, Assistant Professor Dr. Nopadon Muangnoicharoen, and Assistant Professor Dr. Somchai Nakapadungrat, Thesis Evaluation Committee members who contributed to improvements of my thesis by critical comments.

Thanks are also extended to Mr. Akkaneewut Chabangborn and Miss Wasuntra Chairat who gave me support and encouragement. I gratefully acknowledge Dr. Surasak Bamrungwong, my father who proofread and corrected my English in thesis and supported me in every stages and aspects during my thesis studies. Last but not least, I felt deeply appreciated to my family, friends, and other persons that I did not mention who always cheered me up all the time.

CONTENTS

LIST OF TABLES

ศูนย์วิทยทรัพยากร
จุฬาลงกรณ์มหาวิทยาลัย

LIST OF FIGURES

CHAPTER I

INTRODUCTION

Despite the fact that the earthquakes happen around the world and cause many hazards, researching into this field is still difficult and not yet fully understood. An earthquake is a rapid return of elastic strain in the Earth crust. The majority of significant earthquakes usually occur at the zones which were marked as boundaries between tectonic plates in where deformation is concentrated.

From past record, the earthquakes are not randomly distributed over the Earth's surface. They tend to be concentrated in narrow zones. According to the plate tectonic theory, the Earth's surface is divided into a mosaic of moving plates. Boundaries between the plates are actively spreading submarine ridges in the middle of the oceans, subduction zones in ocean trenches or mountain ranges on the continents, or margins where the plates slide past one another. Most of the world's earthquakes occur at plate boundaries.

Many researchers (e.g. Iwakuni et al., 2004; Simons et al., 2007 etc.) claim that it is not well understood how collision of Indian plate to Eurasian plate affects the tectonics in Indo-china peninsula. Thailand is a suitable area for crustal dynamics studies, because Thailand covers wide areas of the Indochina Peninsula. Although Thailand is not located at the plate boundaries, this research will expand the idea as well as initiate the study of the field in this area.

1.1 Statement of Problem

Based on plate tectonics model, crustal deformation is concerned by people around the world as of continental plate movement. More importantly, the Earth's surface near active faults normally deforms before, during and after earthquakes. Optimistically, the understanding of such movement could lead to earthquakes prediction in the future. Active crustal deformation could be observed as relative displacement and movement of points on the Earth's surface; ground tilt, linear and angular strains, and fault slip by using Global Positioning System (GPS) measurements. GPS, as a geodetic

2

measurement, can provide very accurate positions on the earth, at millimeter scale. Thus, GPS can be an excellent tool to measure the active deformation of the crust.
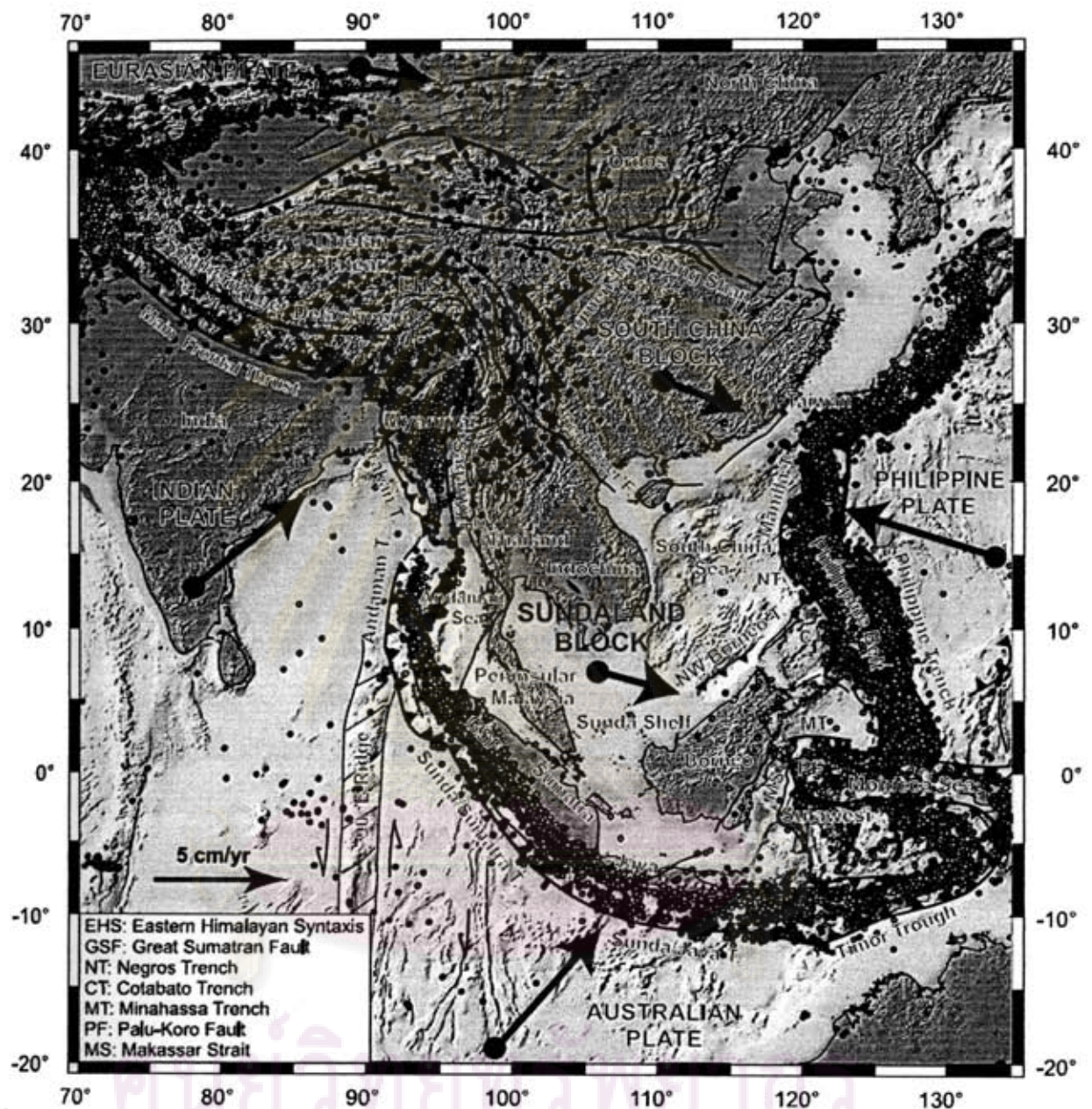
Figure 1.1 Topography, seismicity, main active faults, and the approximate (absolute/ITRF2000) motions of the Eurasian, Indian, Australian, Philippine plates and the South China and Sundaland blocks, respectively, near and in SE Asia (Simons et al., 2007)

The Sundaland block in Eurasian plate shown in Figure 1.1 including mainland Indochina (Vietnam, Laos, Cambodia, Thailand and Malaysia), Sunda shelf, Borneo, Sumatra and Java, is the southeastern extremity of the vast zone of Asian continent affected by the collision between Indian-Australian plate and Asia. Previous studies showed that with respect to Eurasia, Sundaland block moves about 10 millimeters per year eastward, small but noticeable, and while within the block, the deformation is less than 7 microstrain/yr (Simons et al., 2007). Nevertheless, these little changes may indicate an accumulation of elastic stress in the plate. An attempt to understand such geodetic movement is thus needed. Thailand which covers a wide area of the Indochina Peninsula, but slightly far away from the active plate margin, into a somewhat stable zone is therefore considered as a suitable area for crustal dynamics study. In addition, there already were quite a few researches that study in regional aspect in this area. Therefore, it is very interesting to gain a better understanding of the phenomenon in Thailand region.

1.2 Objective

The objective of this research is to study how a portion of Sundaland block, especially Thailand, deforms before and after the 26 December 2004 Sumatra-Andaman mega-earthquake, which will be called "the Boxing-day mega-earthquake", by using GPS measurement and strain analysis.

1.3 Scope of the Investigation

Two periods of GPS data will be focused and analyzed in this study. The details are as below.

1) Before the incident of the Boxing-day mega-earthquake
2) After the Boxing-day mega-earthquake upto 2006.

1.4 Expected Contribution

To gain understanding of the better characteristics of crustal deformation in Thailand during 1994-2006

CHAPTER II
THEORY AND LITERATURE REVIEW

In this chapter theory and literature reviews which are related to this research are discussed. Section 2.1 gives an overview of crustal deformation process and plate tectonics theory. Section 2.2 presents the basic ideas about strain as the path of finding solution in this research. In Section 2.3, the equipment that used for data collection is explained. Finally, Literature Reviews are discussed in Section 2.4.

2.1 Crustal Deformation Process and Plate Tectonics Theory

Deformation of rock involves changing in the shape and/or volume of these substances. Stress is the force applied to material that tends to change its dimensions while strain is the result of stress shown by the material. The response of a rock to stress depends on the type of stress, the amount of pressure, the temperature, the type of rock, and the length of time the rock is subjected to the stress. There are 3 types of deformation in relationship with stress. (Ritter, 2006)

1. Elastic Deformation - Strain is linear proportional to stress. Rock will return to original state if stress is released. (Figure 2.1 or 2.2)

2. Brittle Failure - Any rock will break if the applied stress is to a critical value. Rocks at or near the surface (cold, low pressure) tend to deform by brittle rupture. Results in fracturing and faulting (rock shows differential movement on either side of the fracture surface). (Figure 2.1)
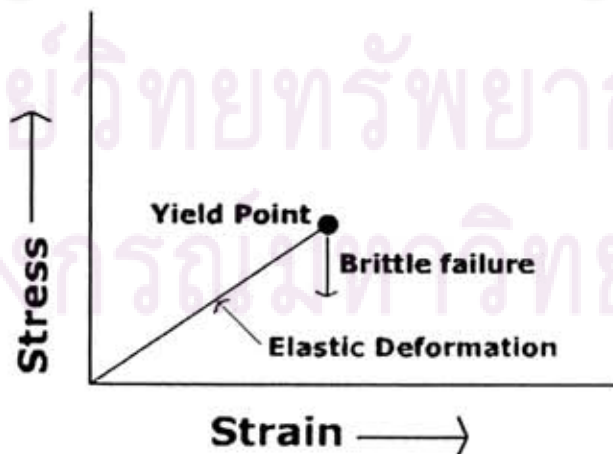
Figure 2.1 Brittle failure (Ritter, 2006)

3. Plastic Deformation - Permanent deformation caused by flowing and folding at stresses above the elastic limit at high confining pressure and/or temperature. Warm rocks tend to deform plastically. (Figure 2.2)
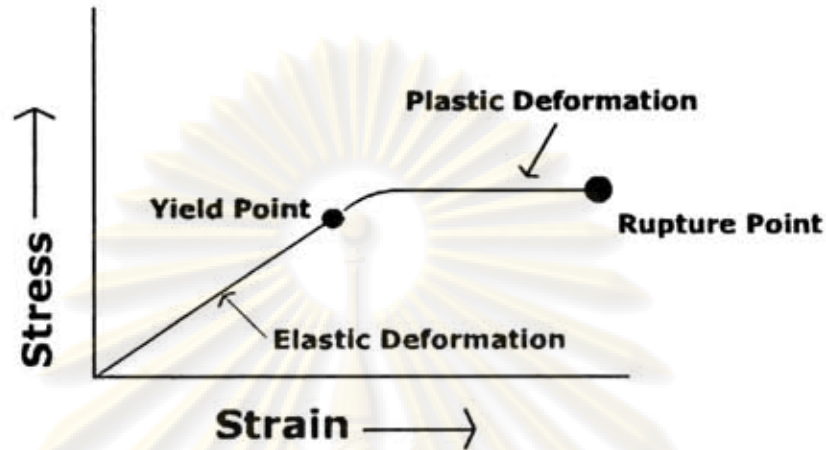
Figure 2.2 Plastic Deformation (Ritter, 2006)

Continuous deformation changes in shape and volume when stress and strain causes rock to buckle and fracture or crumple into folds. A fold can be defined as a bend in rock that is the response to compressive forces. Folds are most visible in rocks that contain layering. (Figure 2.3)
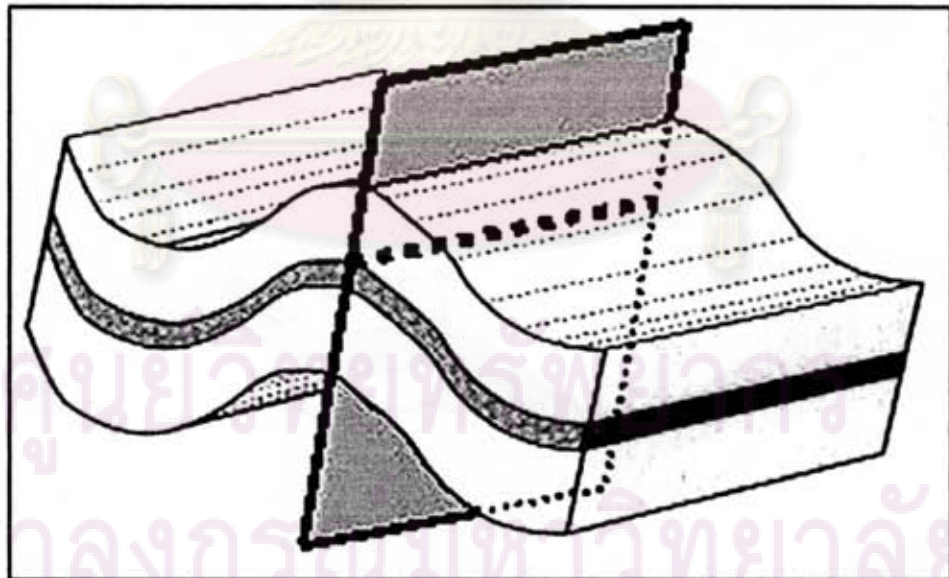
Figure 2.3 The regularity of fold structures can assist with interpolation. This diagram shows the fold axial surface and the hinge line where a geologic formation intersects the axial surface (McInerney et al., 2005).

Discontinuous deformation can occur as faults form in rocks when the stresses overcome the internal strength of the rock resulting in a fracture. There are several different kinds of faults. These faults are named by the nature of the relative movement of the rock blocks across the fault plane thus reflecting the type of stress that acts on the rock. (Pidwirny, 2006) There are three basic types of faults. Normal faults occur when tensile forces act in opposite directions and cause one slab of the rock to be displaced up and the other slab down (Figure 2.4a). Reverse faults develop when compressive forces exist. Compression causes one block to be pushed up and over the other block (Figure 2.4b). Transform or strike-slip faults are faults move in horizontal, one block passing another one (Figure 2.4c).
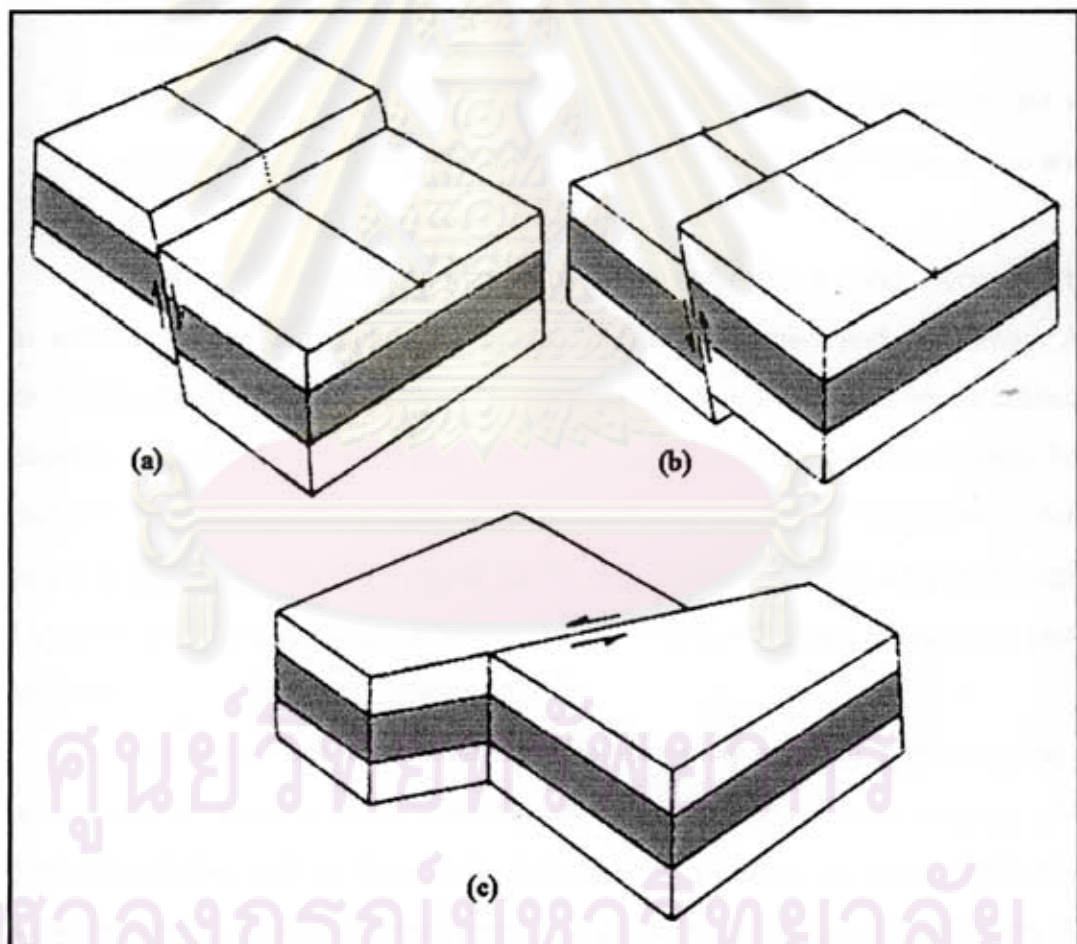
Figure 2.4 Basic classification of fault types: (a) Normal fault, (b) Reverse fault and (c) Strike-slip fault (modified after Jordan, 2006).

Deformation of the Earth's surface is the result of powerful forces which move ocean sediments to an elevation many thousands meters above sea level. Generally speaking, the displacement or deformation of rock can be caused by a tectonic plate movement.

Plate tectonics is a unifying model that attempts to explain about the origin of patterns of deformation in crust, earthquake distribution, supercontinents, and mid-ocean ridges. The theory of plate tectonics combines several ideas about continental drift (originally proposed in 1912 by Alfred Wegener in Germany) and sea-floor spreading (suggested originally by Harry Hess of Princeton University). Two major premises of plate tectonics are as follows (Condie, 2005):

1. The lithosphere behaves as a strong, rigid substance resting on a weaker asthenosphere.
2. The lithosphere is broken into numerous segments or plates that are in motion with respect to one another and are continually changing shape and size.

The Earth's surface is like a mosaic of plates which are moving. According to plate tectonic theory, the plates are being continually created and consumed. At oceanic ridge, adjacent plates diverge from each other in a process known as seafloor spreading, the parental theory of plate tectonics. As the adjacent plates diverge, hot mantle rock ascends to fill the gap. The hot solid mantle rock behaves like a fluid because of solid-state creep processes. As the hot mantle rock cools, it becomes rigid and accretes to the plates, creating new plate area. These are known as divergent plate boundaries.

Because the surface area of the Earth is essentially constant, there must be a complementary process of plate consumption. This occurs at ocean trenches. The plates bend and descend into the interior of the Earth in a process known as subduction. At an ocean trench, the two adjacent plates converge, and one descends beneath the other. For the above reason, ocean trenches are also known as convergent plate boundaries.

The zone between two plates sliding horizontally past one another is called a transform-fault boundary, or simply a transform boundary. These large faults or fracture zones connect two spreading centers (divergent plate boundaries) or, less commonly, trenches (convergent plate boundaries). (Ryan, 2006)

As mentioned all above, there are 3 types of plate boundaries and also major plates on the Earth's surface shown on Figure 2.5 (Condie, 2005):
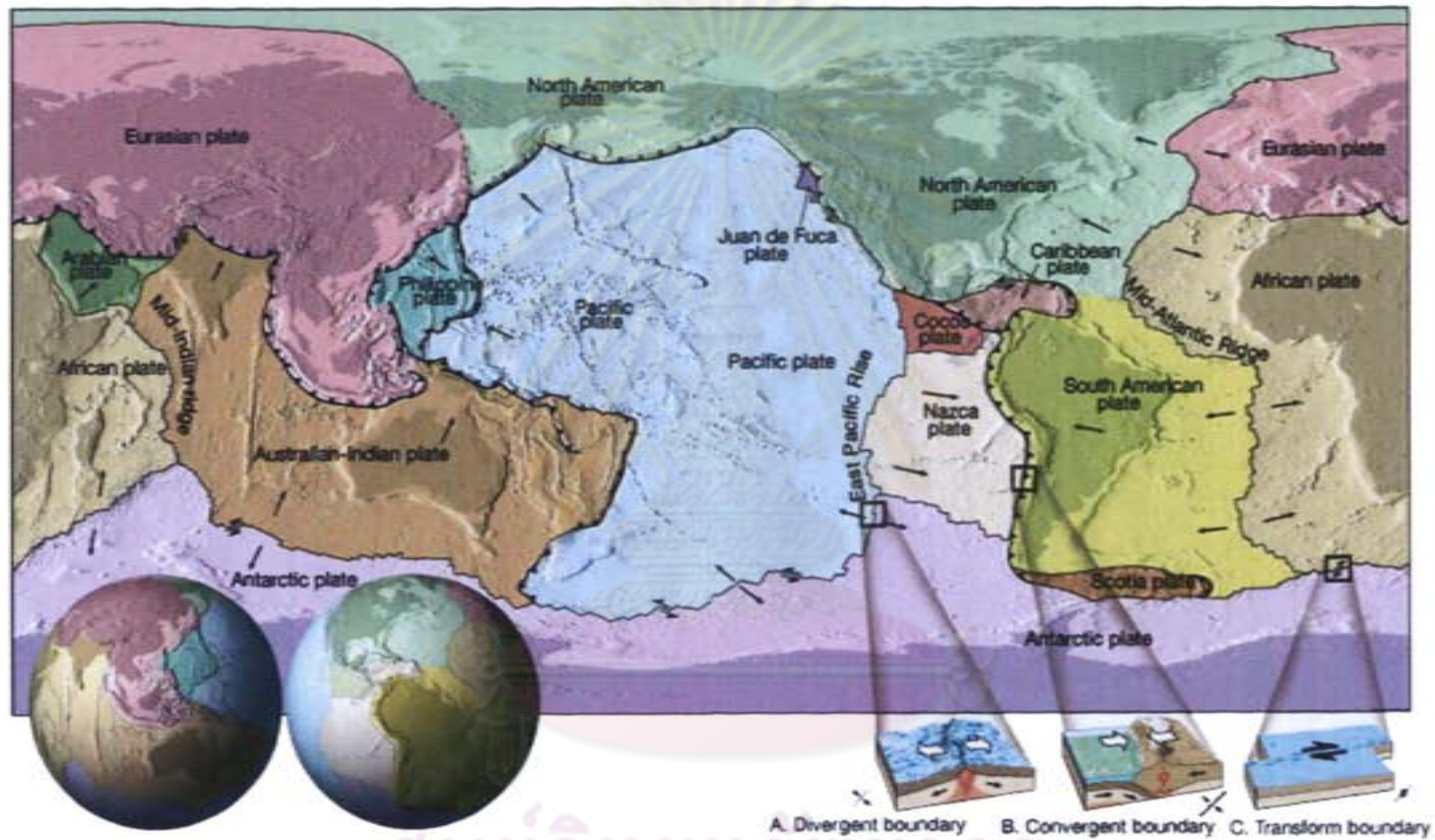
Figure 2.5   Map of the Major lithospheric plates on Earth. Arrows are directions of plate motion. Filled

barbs are convergent plate boundaries (subduction zones and collisional orogens); single

lines are divergent plate boundaries (ocean ridges) and transform faults. Cross-sections

show details of typical plate boundaries. (Artwork by Dennis Tasa courtesy of Tasa

Graphic Arts)

2.2 Basic Ideas about Strain

There are two classes of deformation, namely homogeneous deformation and inhomogeneous deformation. In case of a homogeneous deformation, all parallel lines of particles of material in the undeformed state remain parallel in the same proportion in deformed state. Whereas in an inhomogeneous deformation, vice versa, at least some initial parallel lines become nonparallel, the straight lines becoming curved or broken. However, inhomogeneous deformation though commonly occurred, is more complex to describe than homogeneous deformation, so, in this study, a statistically homogeneous, known as homogeneous deformation is assumed for simple equations.

Any homogeneous deformation has three components: a strain, a rotation and a translation. (Means, 1976) However, geologists usually consider the term strain as deformation of rocks because they often do know the original shape of a body but do not know the original position of the body.

As mentioned earlier, deformation or strain of the solid, which is a result of stress in an elastic solid, is the quantity describing the change in length of each line on the body and describing how adjacent lines on the body slid or sheared past each other. (Means, 1976) Then strain can be classified as (Van der Pluijm and Marshak, 2004)

1. Contractional: resulting in shortening of a region
2. Extensional: resulting in extension of a region
3. Strike-slip: resulting from movement without either shortening or extension.

For quantities expressing length change, the term of elongation, stretch and quadratic elongation are considered. The elongation of a line, sometimes referred to as normal strain, is the ratio of its change in length to a reference length taken as the length of the line in the undeformed state. Then

$$\varepsilon = \frac{l_d - l_u}{l_u} = \frac{\Delta l}{l_u} \tag{2-1}$$

where ε is the elongation and l_d and l_u are the length in the deformed and undeformed (original) state, respectively.

The stretch of a line (S) is the ratio of its deformed to undeformed lengths:

$$S = \frac{l_d}{l_u} = (1 + \varepsilon).$$ (2-2)

The quadratic elongation (λ) is the square of the stretch:

$$\lambda = S^2.$$ (2-3)

For more than one dimension, the decrease in volume accompanying an increase in pressure due to the compressibility of a solid is the simplest example of strain. This volume change is known as volumetric strain or dilation. The volumetric strain or dilation (Δ) is the ratio of volume change to initial volume.

$$\Delta = \frac{V_d - V_u}{V_u} = \frac{\Delta V}{V_u}.$$ (2-4)

For the sake of convenience, infinitesimal strain is considered so the volumetric strain become

$$\Delta = \varepsilon_{xx} + \varepsilon_{yy} + \varepsilon_{zz} = \frac{\partial u}{\partial x} + \frac{\partial v}{\partial y} + \frac{\partial w}{\partial z}$$ (2-5)

which x, y and z denote coordinate axes while u, v and w denote displacements in directions of the axes x, y and z respectively. The subscript xx, yy and zz are referred to normal strain in direction x, y and z, respectively.

Then for quantities expressing shear (or called shear strain) the change in angle occuring between two line segments that were originally perpendicular to one another. Then

$$\gamma = \tan \psi \tag{2-6}$$

where γ is shear strain and ψ is angular change sometime called angular shear. Clockwise shear strains will be negative and anticlockwise shear strains will be positive. Turcotte and Schubert (2002) define the shear strain as one-half of the decrease in a right angle in a solid through which the sides of the original rectangular element are rotated when it is deformed. Then

$$\varepsilon_{xy} \equiv -\frac{1}{2}(\phi_1 + \phi_2), \tag{2-7}$$

where ϕ_1 and ϕ_2 are the angles through which the sides of the original rectangular element are rotated. The sign convention adopted here makes ε_{xy} negative if the original right angle is altered to an acute angle. In the engineering literature (Hibberaler, 1997), $\gamma_{xy} = 2\varepsilon_{xy}$ is often used. Like the volumetric strain, infinitesimal strain equation is considered for shear strain and can be represented as:

$$\varepsilon_{xy} = \frac{1}{2}\left(\frac{\partial v}{\partial x} + \frac{\partial u}{\partial y}\right) \tag{2-8}$$

Shear strain can also lead to a solid-body rotation of the element if $\phi_1 \neq \phi_2$. The solid-body rotation (ω_z) is defined by the following relationship

$$\omega_z \equiv -\frac{1}{2}(\phi_1 - \phi_2) \tag{2-9}$$

or

$$\omega_z = \frac{1}{2}\left(\frac{\partial v}{\partial x} - \frac{\partial u}{\partial y}\right) \tag{2-10}$$
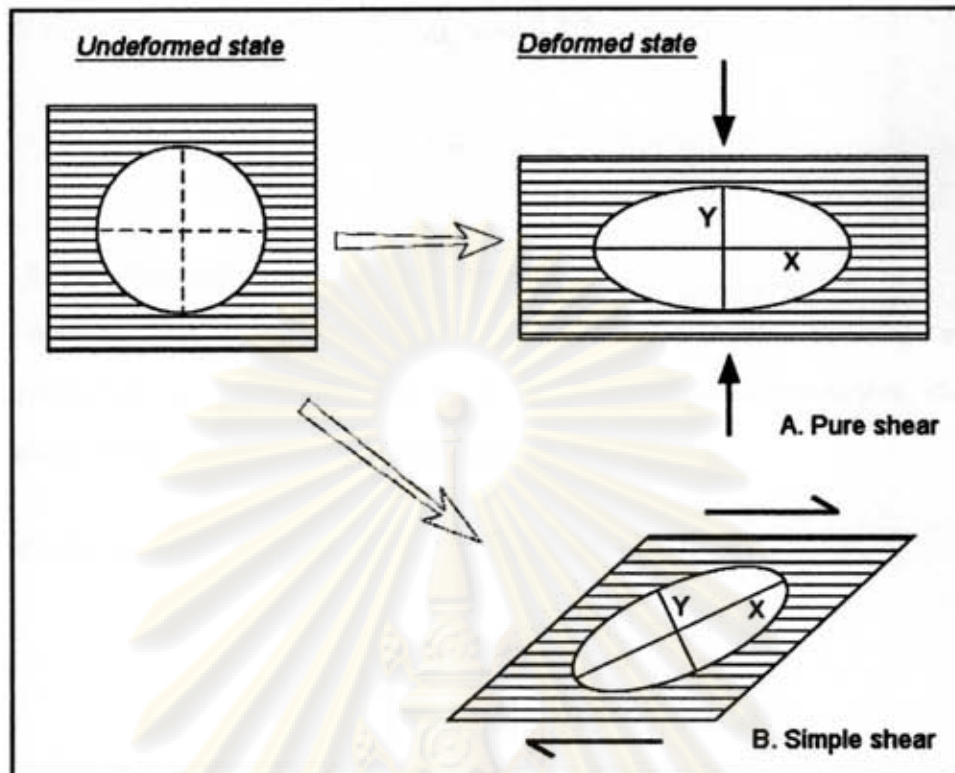
Figure 2.6 An infinitesimal element of a body in undeformed state and deformed state
as A. Pure shear and B. Simple shear (modified after a publication of
Integrated Ocean Drilling Program, IODP)

If the amount of solid-body rotation is zero, known as irrotational deformation, the distortion is called pure shear, illustrated on Figure 2.6A. Then

$$\phi_1 = \phi_2 \tag{2-11}$$

$$\varepsilon_{xy} = \frac{\partial v}{\partial x} = \frac{\partial u}{\partial y} \tag{2-12}$$

The case of simple shear, shown in Figure 2.6B, is the combination of rotation component and shear strain component in such a manner that

$$\phi_1 = \frac{\partial v}{\partial x} = 0 \tag{2-13}$$

Then
$$\omega_z = -\frac{1}{2}\frac{\partial u}{\partial y}$$
(2-14)

and
$$\varepsilon_{xy} = \frac{1}{2}\frac{\partial u}{\partial y}.$$
(2-15)

2.2.1 Principal strain in two dimensions

Because the strain tensor is a real symmetric matrix, by singular value decomposition it can be represented as a set of orthogonal eigenvectors, directions along which there is no shear, only stretching or compression.

Assuming the two dimensional strain tensor given as:

$$\varepsilon_{ij} = \begin{bmatrix} \varepsilon_{xx} & \varepsilon_{xy} \\ \varepsilon_{xy} & \varepsilon_{yy} \end{bmatrix}$$
(2-16)

Then principal strains $\varepsilon_1, \varepsilon_2$ are equal to the eigenvalues of ε :

$$\varepsilon_1 = \frac{\varepsilon_{xx} + \varepsilon_{yy}}{2} + \sqrt{\frac{(\varepsilon_{xx} - \varepsilon_{yy})^2}{4} + \varepsilon_{xy}^2}$$
(2-17)

$$\varepsilon_2 = \frac{\varepsilon_{xx} + \varepsilon_{yy}}{2} - \sqrt{\frac{(\varepsilon_{xx} - \varepsilon_{yy})^2}{4} + \varepsilon_{xy}^2}$$
(2-18)

In the principal strain axis coordinate system, shear strain components are zero. The direction of one of the principal axes of strain as

$$\tan 2\theta = \frac{2\varepsilon_{xy}}{\varepsilon_{xx} - \varepsilon_{yy}}.$$
(2-19)

where θ is an angle between the direction of maximum variance and x-direction.

2.2.2   The Strain Ellipse

In any homogenous deformation, particles lying on the surface of a sphere in the undeformed state will lie on the surface of an ellipsoid in the deformed state. This ellipsoid is called the strain ellipsoid. Like any ellipsoid, the general strain ellipsoid has three planes of symmetry at right angles to one another. These planes intersect in the three principal diameters of the ellipsoid, and the directions of these diameters are called the principal directions of strain (or principal strain).

Strain ellipsoid, which usually display in two dimensions as in Figure 2.7, can be an application of showing the development of fault, fold and/or other geological structure.
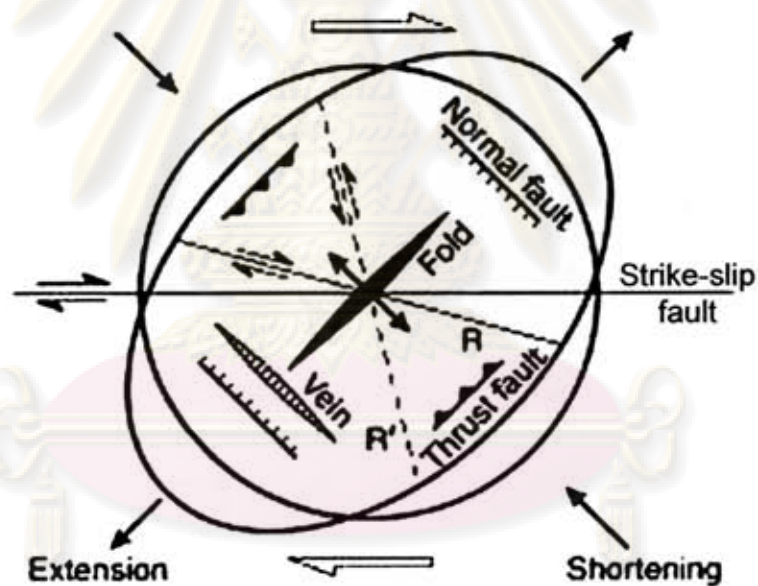
Figure 2.7 A detail of the strain ellipse showing that folds and thrusts form perpendicular to the shortening direction, while normal faults and veins form perpendicular to the extension direction. R and R′ shears form at an acute angle to the shortening direction. (modified after Van der Pluijm and Marshak, 2004)

2.2.3 Strain Measurements

The surface of the Earth, which is continually being strained by tectonic processes, is often a consequence of large-scale forces. Hence, the measurement of surface strain can provide important information on fundamental geodynamic processes. Because surface strains are generally very small, sophisticated distance-measuring techniques are required to determine them. Thus geodetic techniques, especially GPS, can measure these changes in strain. By using geodetic networks, a triangle is the minimum polygon to compute strain. Figure 2.8 shows the deformation possibly happening when strain is analyzed by geodetic network.

For the long term analysis, strain rate per year are usually determined. The velocity field is used to analyze in the same way of the displacement field.
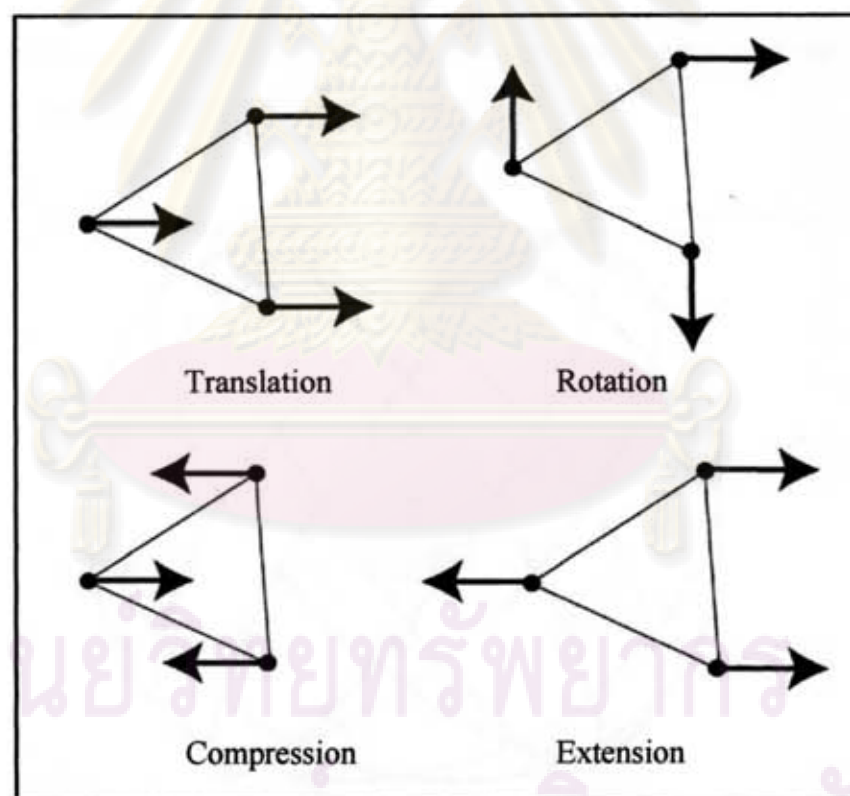
Figure 2.8 Types of deformation that possibly happens in each triangle. Each red dot represents point that measure displacement or velocity represented by black arrows.

2.3 Basic concept of GPS

The Global Positioning System (GPS) is a satellite-based navigation system which is funded and controlled by the U.S. Department of Defense (DOD) and is now only fully functional Global Navigation Satellite Systems (GNSS). To compute position in three dimensions and the time offset in the receiver clock, it requires at least four GPS satellites. GPS system consists of three segments: the space segment, the control segment, and the user segment.

2.3.1 Space Segment

The space segment currently consists of nominal 28 GPS satellites (on September 10th, 2008) that orbit the earth at an altitude of approximately 20,200 kilometers in six circular orbital planes, shown in Figure 2.9, which have approximately 55 degree inclination (relative to Earth's equator) and equally spaced (60 degrees apart), with four satellites each in 12 hours. This constellation provides the user with between five and eight satellites visible from any point on the earth.

Figure 2.9 GPS Satellite Obits (Dana, 2000)

Each GPS satellite continually transmits a signal which has components i.e. two sinusidal waves (also known as carrier frequencies, L1=1,575.42 MHz and L2=1,227.60 MHz), two digital codes (C/A-code and P-code), and a navigation massage which

contains the time the message was sent, an orbit information for the satellite sending the message (the ephemeris), and the general system health and rough orbits of all GPS satellites (the almanac). The carriers and the codes are used mainly to determine the distance from the user's receiver to the GPS satellites. (Figure 2.10)
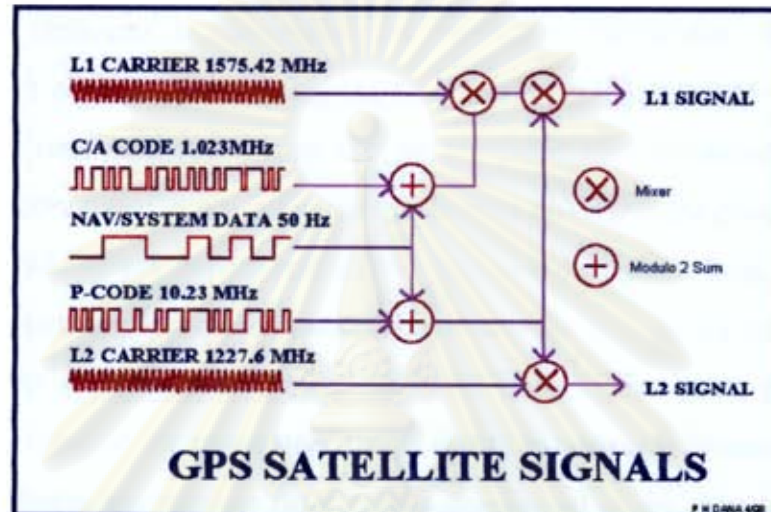
Figure 2.10 GPS Satellite Signals (Dana, 2000)

2.3.2 Control Segment

US Air Force monitoring stations in Hawaii, Kwajalein, Ascension Island, Diego Garcia, and Colorado Springs, which are the control segment of the GPS system, have a primary task to track the GPS satellites in order to determine and predict satellite locations, system integrity, behavior of the satellite atomic clocks, atmospheric data, the satellite almanac, and other considerations. The Master Control station, locating at Schriever Air Force Base (formerly Falcon AFB) in Colorado, uploads ephemeris and clock data to the satellite.

2.3.3 User Segment

The GPS User Segment, including all military and civilian users, consists of the GPS receivers and the user community. GPS receivers can receive the GPS signals which can be converted into position anywhere in the world. GPS is currently available to all users worldwide at no direct charge. There are a number of the usage of GPS data

such as navigation, positioning, time dissemination, and research. Plate tectonic studies are also an example of research using precise positioning of GPS receivers.

2.3.4 Concept of Positioning using GPS Measurements

The basic principle of the absolute positioning technique is to use simple resection by distances to determine the receiver's coordinates. If the satellite coordinates are assumed to be know (as they can be computed from the navigation message), the receiver's coordinates can be computed from the resection using the measured pseudoranges. If it is assumed that there is no error in the pseudoranges, the absolute coordinates are considered as the only unknown parameters. Therefore, at least three pseudoranges need to be measured in order to solve for three coordinate components. As a matter of fact, there are many errors in measuring pseudoranges, especially in measuring the travel time. This is due to the use of an inexpensive clock in the receiver. Hence, the receiver clock bias is considered as an additional parameter, and a minimum of four pseudoranges are then needed to solve for four unknown parameters, three coordinates and the receiver clock offset. (Satirapod, 2002)

2.4 Literature Review

Since 1990's, GPS networks in Southeast Asia have been established by several projects such as GEODYSSEA (GEODYnamics of South and South-East Asia), GAME-T (GEWEX Asia Monsoon Experiment Tropics) and SEAMERGES (South-East Asia Mastering Environmental Research with GEodetic Space techniques). Thus, there were some experiments had started before the 2004 great Sumatra-Andaman earthquake. As in 1994 and 1996, Chamot-Rooke and Le Pichon (1999) used GPS measurements over Southeast Asia under the framework of the GEODYSSEA program to reveal that a large piece of continental lithosphere comprising the Indochina Peninsula, Sunda shelf and part of Indonesia behaves as a rigid 'Sundaland' block. A direct adjustment of velocity vectors obtained in a Eurasian frame of reference showed that Sundaland block was rotating clockwise with respect to Eurasia around a pole of rotation located at the southern part of Australia. After that, Michel et al. (2000) repeated GEODYSSEA-GPS measurements and added more GPS data from the International GPS Service (IGS) and Asia Pacific Regional Geodetic Project (APRGP) 97/98 to constrain the motion of SE-Asia within a global reference frame. They found that Sundaland and South China were moving coherently to the east along the boundaries, and that the eastward motion of India was compensated by the eastward motion of Sundaland-South China. In addition, they indicated that Sundaland, i.e. Indochina along with the western and central part of Indonesia, constituted a stable tectonic block moving approximately east with respect to Eurasia at a velocity of 12±3 millimeters per year (Michel et al., 2001)

Considering a regional aspect, Vigny et al. (2003) used GPS measurement campaigns in Myanmar, conducted in 1998 and 2000, to quantify the present-day crustal deformation around the Sagaing fault system in central Myanmar. They found that active deformation related to the northward motion of India is distributed across Myanmar in a block that extends from the western edge of Shan Plateau in the east to the Andaman Trench in the west. For Thailand, Iwakuni et al. (2004) tried to elucidate the deformation on the peninsula by using six permanent GPS sites which were established in Thailand and had been conducted since March 1998. They found that the strain rate

in the order of 10^{-8} per year, small but significant, existed in Thailand and estimated velocities suggested that most of the Indochina peninsula was rigid.

After the incident of the 26 December 2004 Sumatra-Andaman earthquake, Vigny et al. (2005) found that the rupture plane for this earthquake must be at least 1000 kilometers long and that non-homogeneous slip was required to fit the large displacement gradients revealed by the GPS measurements which were collected at about 60 sites in Southeast Asia. Furthermore, Hashimoto et al. (2006) had analyzed continuous GPS data from more than 20 sites in Asia, Australia and islands in Indian Ocean. It was found that large post-seismic displacements were observed at Phuket and Sampari after the mainshock and the spatial distribution of afterslip was different from the co-seismic slip distribution. In Thailand, Satirapod, Simons et al. (2007) determined the post-seismic displacements from the GPS campaigns which collected the data in January 2005 and February 2005 and found that the earthquake had resulted in the horizontal displacements, ranging from 33 cm in the south, 9 cm in the centre, to about 3 cm in the north and east of Thailand. Moreover, the post-seismic motion due to the earthquake had increased further the displacement at the PHUK (Phuket) station. For the following earthquake, the Nias earthquake, Satirapod, Laoniyomthai and Chabangborn (2007) found the impact that the earthquake had resulted in small horizontal displacements in the central and southern parts of Thailand.

According to the finding in the above-mentioned publications, the crustal deformation in Thailand in the view of strain rate tensor is still not considered. Therefore, it is interesting to pursue research in this point.

CHAPTER III
METHODOLOGY AND DATA USED

The methodology as well as the data used in this research will be explained in this chapter. Section 3.1 discusses about the methodology and the steps involving the derivation of strain rate. In Section 3.2, data collection and equipment used are described. Data processing is discussed in Section 3.3.

3.1 Methodology

After conversing raw GPS data to GPS RINEX format, the GPS RINEX files were processed using the GIPSY-OASIS II software to obtain coordinates for each GPS station. To get the strain rate tensors in horizontal, coordinates, displacements and velocities were calculated based on the assumption that inside of each triangle which was calculated by 3 stations is homogeneous. Then the derived displacements and velocities were used as input to produce the strain rate tensors before the Sumatra-Andaman earthquake occurrence about 10 years (1994 – 2004) and 1.5 months after the Sumatra-Andaman earthquake and every 3 months after Nias earthquake up to November 2006. Figure 3.1 presents a flow chart of the research methodology.
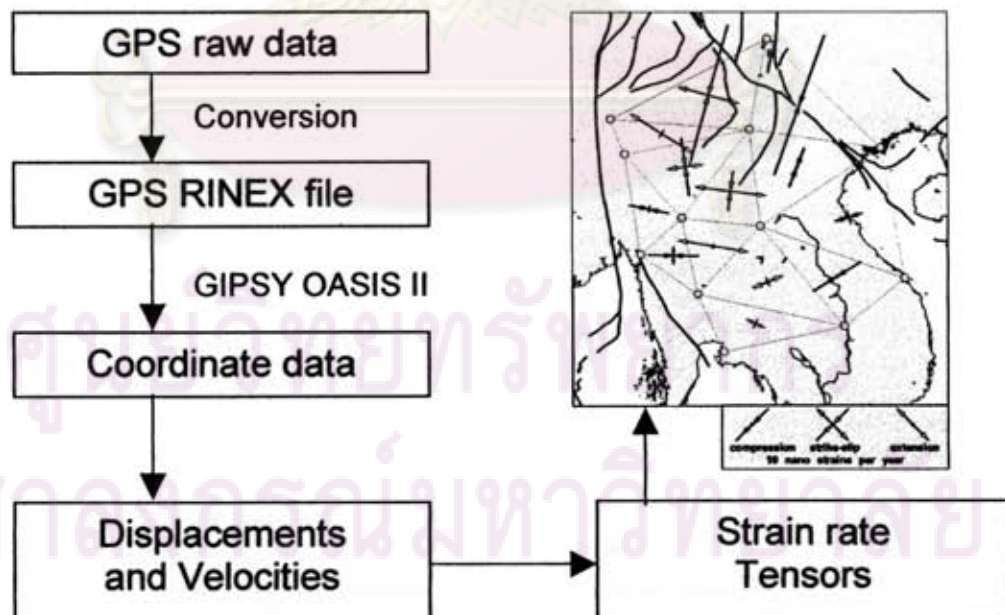
Figure 3.1 Methodological flow chart

3.2 Data Collection and Equipment Used

The primary GPS data used in this research were kindly provided by the Royal Thai Survey Department and International GNSS Service (IGS).

The GPS data obtained from the Royal Thai Survey Department (RTSD), which have been regularly measured since 1994. A total of 5 GPS stations, Chumporn (BANH), Chonburi (CHON), Uthaitani (UTHA), Srisaket (SRIS), and Lampang (OTRI) were used in this study. Location and the availability of GPS data of each GPS sites in Thailand can be seen in Table 3.1 and Table 3.2 respectively.

In addition, the data from a station (GETI) as a part of IGS network, which is a voluntary federation of many worldwide agencies that pool resources and permanent GNSS station data to generate precise GNSS products. The GETI station will fulfill the gap in the southern part of Thailand and lead to a more comprehensive study of deformation over Thailand region.
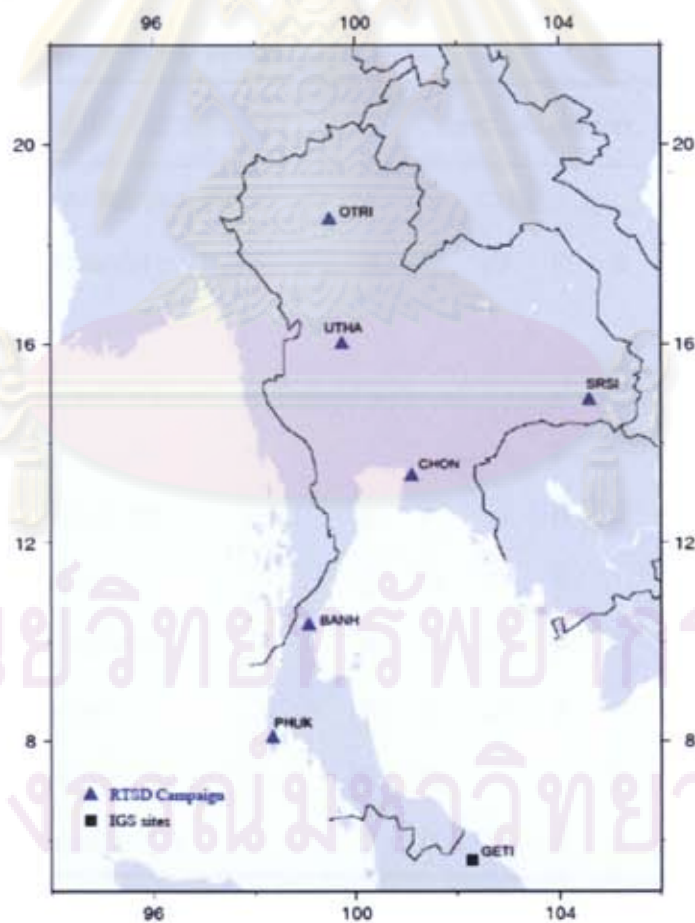
Figure 3.2 GPS Sites in Thailand and northern Malaysia used in this study

Table 3.1 Location of GPS sites collecting data in this research

GPS Station Name	Location	Longitude (°N)	Latitude (°E)
PHUK	Phuket	98.304	7.759
BANH	Chumporn	99.076	10.61
CHON	Chonburi	101.045	13.121
UTHA	Uthaitani	100.013	15.384
SRIS	Srisaket	104.416	14.901
OTRI	Lampang	99.371	18.335
GETI	Geting, Malaysia	102.105	6.226

Table 3.2 Availability of GPS data observed at the Thai geodetic network sites (Satirapod et al., 2008)

GPS Campaign	Observed station					
Before earthquake						
October-04	B	C	O	P	S	U
After earthquake						
January-05				P		
February-05	B	C	O	P	S	U
July-05	B	C	O	P	S	U
October-05	B	C	O	P	S	U
April-06	B	C	O	P	S	U
July-06	B	C	O	P	S	U
November-06	B	C	O	P	S	U

(Note: B = BANH, C = CHON, O = OTRI, P = PHUK, S = SRIS and U = UTHA)

3.3 Data Processing

3.3.1 Calculation of coordinate time series from GPS measurements

After conversion of GPS raw data to RINEX files (standard GPS data format), the RINEX files and additional data are processed by GPS Inferred Positioning System-Orbit Analysis and Simulation Software or GIPSY-OASIS II which is software processing as the GPS Precise Point Positioning (PPP) technique as each individual station needs to be determined the magnitude of displacement as a real picture.

The additional information required for GPS data processed by GIPSY-OASIS II are the JPL precise orbits, information of time, polar motion and earth orientation as well as satellite eclipse information. They can be downloaded from Jet Propulsion Laboratory (ftp://sideshow.jpl.nasa.gov). The individual PPP station coordinate solutions were computed using the ionosphere-free linear combination of the zero-differenced GPS phase and pseudorange data at 5 minute intervals with an elevation cut-off angle of 15 degrees. To account for tropospheric effects, the zenith path delay and gradients are estimated at each time interval. Data from GPS satellites that were undergoing maintenance during part of the processed day (ftp://tycho.usno.navy.mil/pub/gps/) were removed. Ocean loading modeling parameters for all site locations were obtained from Onsala Space Observatory website (http://www.oso.chalmers.se/~loading/). Finally, because different antennae were used in the network, the NGS relative antenna phase center corrections (http://www.ngs.noaa.gov/ANTCAL) were applied. (Simon et al., 2005)

In a final processing step, all individual solutions are merged into one daily covariance band matrix (no correlations between different stations), after which the ambiguities can be resolved. In addition, due to the widespread deformation, a local or national reference frame cannot be used to present the latest coordinates and displacements. Therefore, a number of permanent GPS stations from the International GPS Service (IGS) need to be included, so that the positioning results can be given in the global International Terrestrial Reference Frame (ITRF) solution of 2000. Previous experience with mapping local networks in South East Asia (e.g. Wilson et al., 1998; Simons et al., 1999; Michel et al., 2001) into ITRF has shown that if only regional IGS stations are selected the mapping may not always be optimal, and position and velocity

errors may occur. Moreover, some stations may have been affected by nearby earthquakes, and hence they do not always fit the linear velocity trend given by ITRF, nor are official position jumps yet made available. To avoid the above-mentioned mapping problems, a number of well-determined global IGS sites are included in the data processing. This is done to establish an un-deformed reference solution, which is not affected by episodic jumps in the time-series of some of the IGS stations. In total, IGS data from 31 stations were retrieved for each campaign period from the IGS databases (Beutler et al., 1994). However, coordinate time series in this research was processed by Dr. Wim Simons of Delf University of Technology (Simon et al., 2005 and 2007) and Dr. Chalermchon Satirapod of Department of Survey Engineering, Chulalongkorn University (Satirapod et al., 2007 and 2008).

To fit coordinate time series of data before the Boxing-day megaearthquake (1994 – 2004), these can be estimated by computing a linear fit through all ITRF-2000 mapped station coordinates and checking the coordinate residuals at each point in the time series (Simon el al., 2007). Whereas fitting coordinate time series of data after the Boxing-day megaearthquake, afterslip events cannot be done using a simple linear trend fitting as done with the time series before the Boxing-day megaearthquake because of continuing deformation. Satirapod et al. (2008) found that a Logarithmic decay function which has been presented by Marone et al. (1991) can fit the postseismic time series due to the 2004 Mega and 2005 Nias earthquakes better. Then the Logarithmic decay function was used to fit displacement of the sites as following: (See best-fit logarithmic model parameters in Appendix A)

$$u(t) = c + a\ln(1 + \frac{t}{\tau_{\log}}) \qquad (3\text{-}1)$$

where t is time since Sumatra – Andaman Earthquake

$u(t)$ is the displacement (east, north, and up)

c is co-seismic offset

a is the amplitude associated with the decay

$\tau_{\log}$ is the logarithmic decay time

3.3.2 Calculation of velocity

As the data fitting as linear during 1994 – 2004, trend line in each station figure is estimated by the plotting software. The uncertainties of all velocity components are at the 95% confidence level.

To find velocities after the Great earthquake, Equation (3-1) from Section 3.3.1.2 has been differentiated by time to get the instantaneous velocity in each station as

$$Velocity = \frac{a}{\tau_{\log} + t} \tag{3-2}$$

3.3.3 Calculation of strain rate tensors

After that, the strain in horizontal has been calculated as 6 minor triangle networks (as shown in Figure 3.3), as divided into 2 periods: one, 1.5 months after Sumatra – Andaman Earthquake (t=0.125) and every three month after Nias Earthquake i.e. t= 0.5, 0.75, 1, 1.25, 1.5, 1.75.

$$
\begin{bmatrix} V_{E1} \\ V_{N1} \\ V_{E2} \\ V_{N2} \\ V_{E3} \\ V_{N3} \end{bmatrix}
=
\begin{bmatrix}
1 & 0 & \Delta E_1 & \Delta N_1 & 0 & 0 \\
0 & 1 & 0 & 0 & \Delta E_1 & \Delta N_1 \\
1 & 0 & \Delta E_2 & \Delta N_2 & 0 & 0 \\
0 & 1 & 0 & 0 & \Delta E_2 & \Delta N_2 \\
1 & 0 & \Delta E_3 & \Delta N_3 & 0 & 0 \\
0 & 1 & 0 & 0 & \Delta E_3 & \Delta N_3
\end{bmatrix}
\begin{bmatrix}
V_{EB} \\ V_{NB} \\ \dfrac{\partial V_E}{\partial E} \\ \dfrac{\partial V_E}{\partial N} \\ \dfrac{\partial V_N}{\partial E} \\ \dfrac{\partial V_N}{\partial N}
\end{bmatrix}
\tag{3-3}
$$

whereas V_{Ei} and V_{Ni} are velocities of stations, i = 1, 2, 3

                  V_{EB} and V_{NB} are velocities at centroid

                  ΔE_i and ΔN_i are coordinate difference at stations, i = 1, 2, 3

In this research, the vertical positioning results does not show any detectable vertical motions in Thailand as their values are within the vertical displacement inaccuracies.
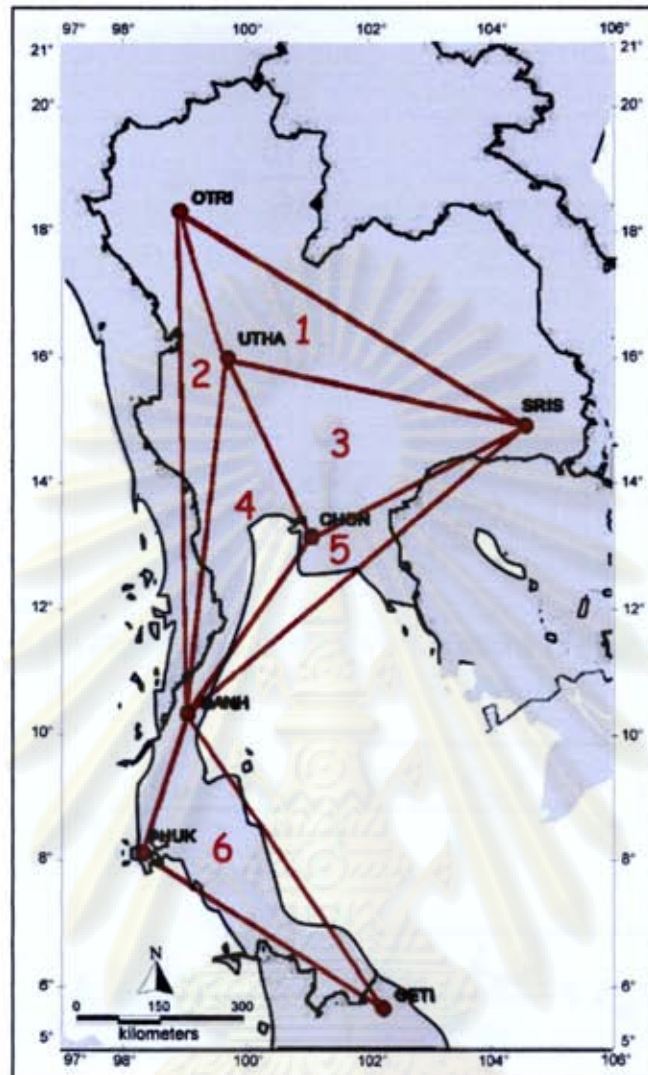
Figure 3.3 The GPS station networks. Numbers 1-6 denote triangular form by 3 nearest stations

From calculated velocity gradient tensors Two-dimensional symmetric strain tensor can be computed from the equation (Cai and Grafarend, 2006)

$$
\mathbf{E} = \begin{bmatrix}
\dfrac{\partial v_E}{\partial E} & \dfrac{1}{2}\left(\dfrac{\partial v_E}{\partial N} + \dfrac{\partial v_N}{\partial E}\right) \\
\dfrac{1}{2}\left(\dfrac{\partial v_N}{\partial E} + \dfrac{\partial v_E}{\partial N}\right) & \dfrac{\partial v_N}{\partial N}
\end{bmatrix}
\tag{3-4}
$$

Each component can be substituted as

$$\dot{\varepsilon}_{xx} = \frac{\partial V_E}{\partial E}$$ (3-5)

$$\dot{\varepsilon}_{yy} = \frac{\partial V_N}{\partial N}$$ (3-6)

$$\dot{\varepsilon}_{xy} = \frac{1}{2}\left(\frac{\partial V_E}{\partial N} + \frac{\partial V_N}{\partial E}\right)$$ (3-7)

which Matrix $\mathbf{E}$ has two Eigenvalues as shown in Equations (3-8) and (3-9)

$$\dot{\varepsilon}_1 = \frac{\dot{\varepsilon}_{xx} + \dot{\varepsilon}_{yy}}{2} + \sqrt{\frac{(\dot{\varepsilon}_{xx} - \dot{\varepsilon}_{yy})^2}{4} + \dot{\varepsilon}_{xy}^{\ 2}}$$ (3-8)

$$\dot{\varepsilon}_2 = \frac{\dot{\varepsilon}_{xx} + \dot{\varepsilon}_{yy}}{2} - \sqrt{\frac{(\dot{\varepsilon}_{xx} - \dot{\varepsilon}_{yy})^2}{4} + \dot{\varepsilon}_{xy}^{\ 2}}$$ (3-9)

where $\dot{\varepsilon}_1$ and $\dot{\varepsilon}_2$ are strain in the direction of compression or extension. Positive value will be considered as extension while negative value as compresstion.

In the principal strain axis coordinate system, shear strain components are zero. The direction of one of the principal axes of strain can be computed using

$$\tan 2\theta = \frac{2\dot{\varepsilon}_{xy}}{\dot{\varepsilon}_{xx} - \dot{\varepsilon}_{yy}}$$ (3-10)

where θ is an angle between the direction of maximum variance and the eastern direction.

After processing the GPS data and calculating the strain rate tensors using the methodology described in chapter III, the results will be presented in this chapter. This chapter comprise of 4 sections: (1) coordinate time series, (2) velocity vectors, (3) strain rate tensors and (4) the discussion of results.

4.1 Coordinate Time Series

4.1.1   Before the Boxing-day mega-earthquake (during 27 Nov. 1994 and 25 Dec. 2004)

During 1994 – 2004, all GPS sites had similarity in changing of position. The time series of CHON site have been selected to present in Figure 4.1. For other stations, please see Appendix C. In summary, each station moved to south in latitude direction, to east in longitude direction and almost every station had slightly uplifted, about 2 - 5 mm per year. Only Lampang (OTRI) site moved differently. The data had a linear trend as the best fit to all sites in all 3 directions.
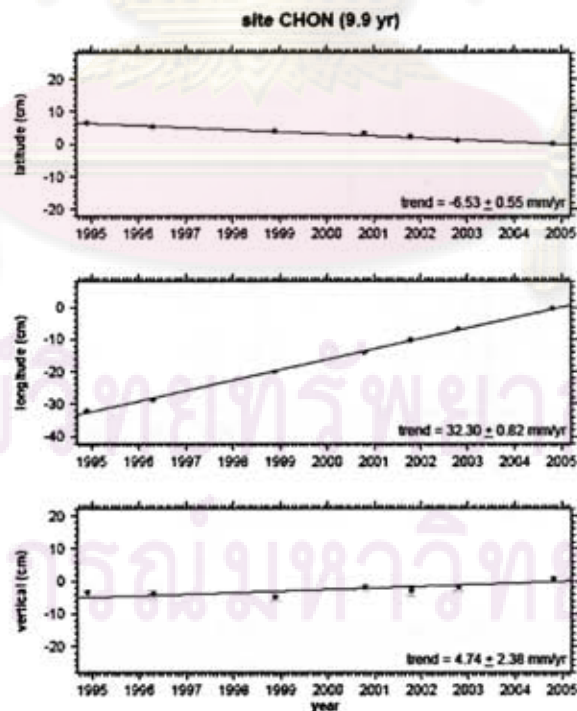
Figure 4.1 Sample of coordinate time series in the period of1994 – 2004: Chonburi (CHON) site (Simons et al., 2007)

4.1.2   After the Boxing-day mega-earthquake (between 26 Dec. 2004 and 6
        Nov. 2006)

After the Boxing-day mega-earthquake, there was a significant movement all
over the region near the epicenter as well as in Thailand. Every station in this research
moved differently from before the occurrence of the earthquake. Each station rapidly
moved to south and west in early stage but moved slowly to the same directions when
the time passed.

It was noted that the Nias earthquake, occurring on 28 March 2005, affected the
southern region of the country mostly. The PHUK (and GETI, not shown in this figure)
movement showed a sudden shift on the date. The Nias event was perhaps a major
aftershock of the mega-earthquake. This post-seismic motion can be fitted very well with
logarithmic decay function as displayed in Figure 4.2
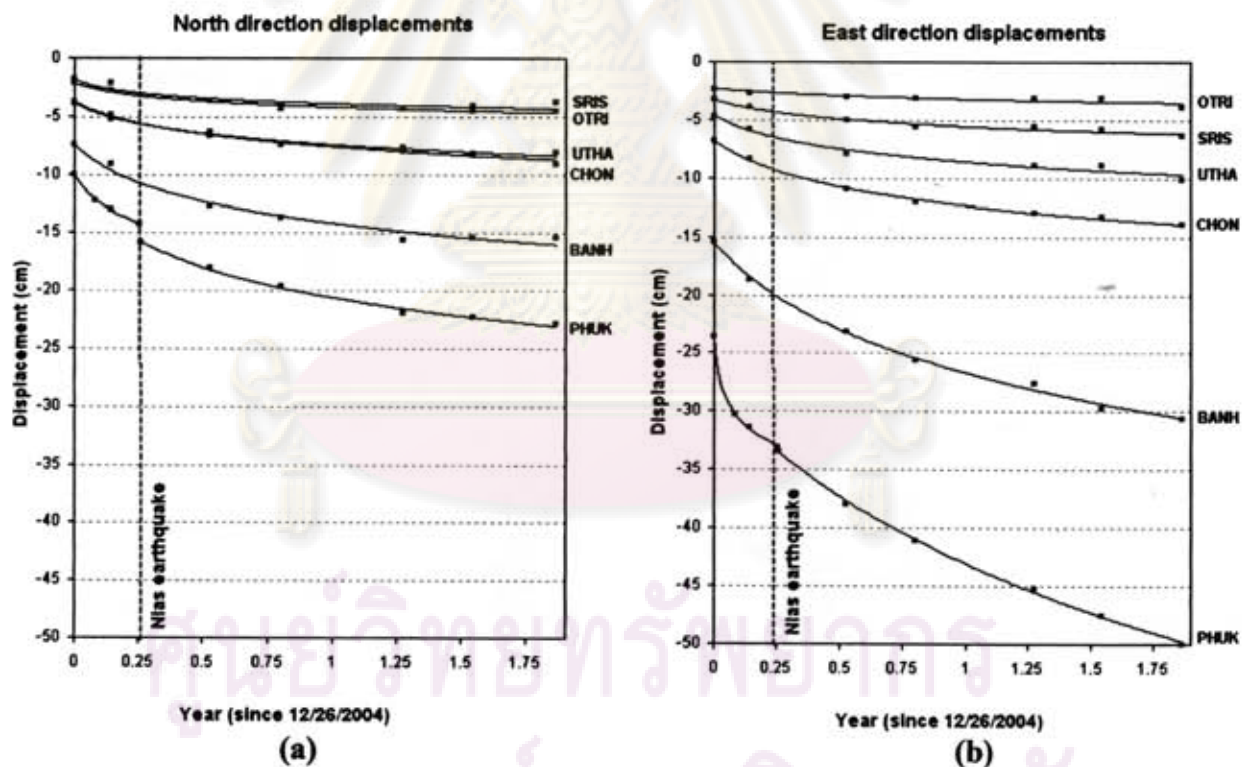
Figure 4.2 Post-seismic time series in north (a) and east (b) direction due to the Boxing-
            day and Nias earthquakes for Thai geodetic network sites. Solid lines are
            best-fit logarithmic decay functions. (Satirapod et al., 2007)

4.2 Velocity Vectors

From coordinate time series, the velocity vectors could be clearly illustrated. To analyze velocity of GPS stations, the time series can be divided into 3 periods – the first period is between 1994 and 2004 (before the Boxing-day mega-earthquake), the second period is between 26 December 2004 and 28 March 2005 (after the Boxing-day mega-earthquake but before the Nias earthquake) and the last period is after 25 March 2005 (after the Nias earthquake).

4.2.1   Before the Boxing-day mega-earthquake (between 27 Nov. 1994 and 25 Dec. 2004)

Velocity vectors in Figure 4.3 were constructed from coordinate time series of Simon et al. (2007) before the Boxing-day mega-earthquake. It was found that each station moved to the same directions, i.e. in the east-southeastern direction. The magnitudes of the vectors are nearly the same, on an average of around 33.2 ± 1.1 millimeter/year.
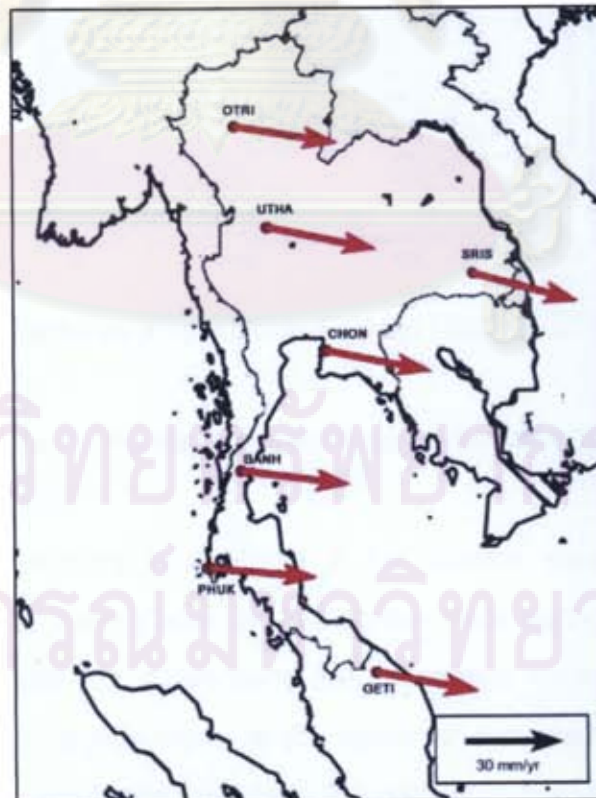
Figure 4.3 Velocity vectors of GPS sites during 1994-2004

The derived velocity vectors were also compared with the results produced by Iwakuni (2004) (Figure 4.4) to be noted that they were very much agreeable as they showed nearly the same direction of movement with the velocity 31 to 35 millimeters per year.
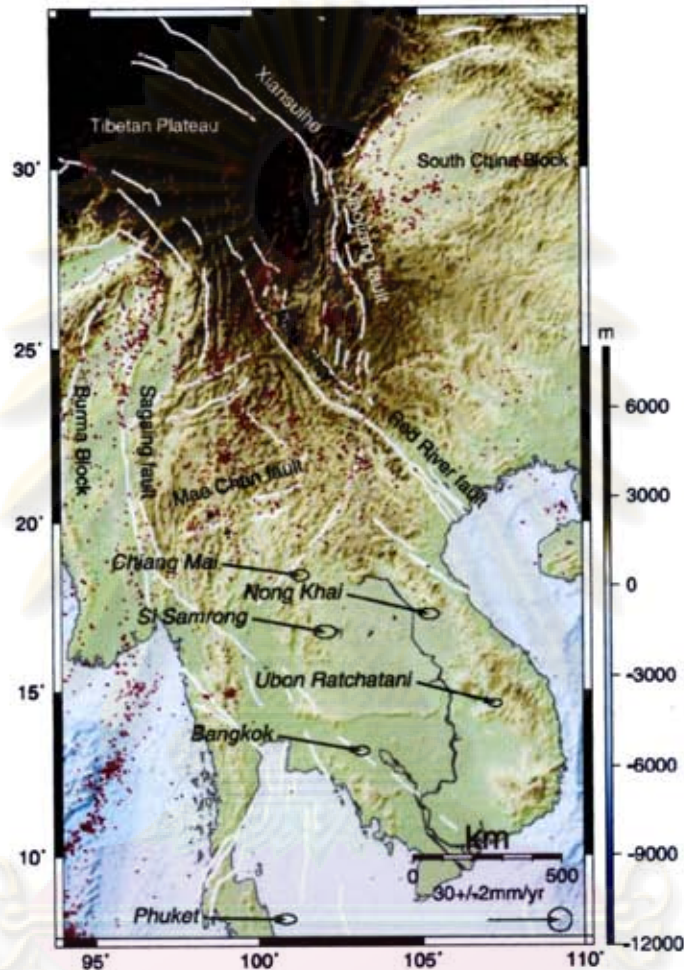
Figure 4.4 Velocity Estimates (ITRF2000) in Thailand (1998-2002) (Iwakuni et al., 2004)

4.2.2   After the Boxing-day mega-earthquake (Between 26 Dec. 2004 and 28 Mar. 2005)

The velocity vectors at one and a half months were calculated as the representatives of the velocity after the Boxing-day mega-earthquake but before the Nias Earthquake (Figure 4.5). It was found that the stations moved in the southwestern direction with greater velocity closer to the epicenter and gradually reduced further away. The velocity at PHUK site was about 240 millimeters per year while that in ORTI site, about 1800kms due north, was only about 40 millimeters per year.
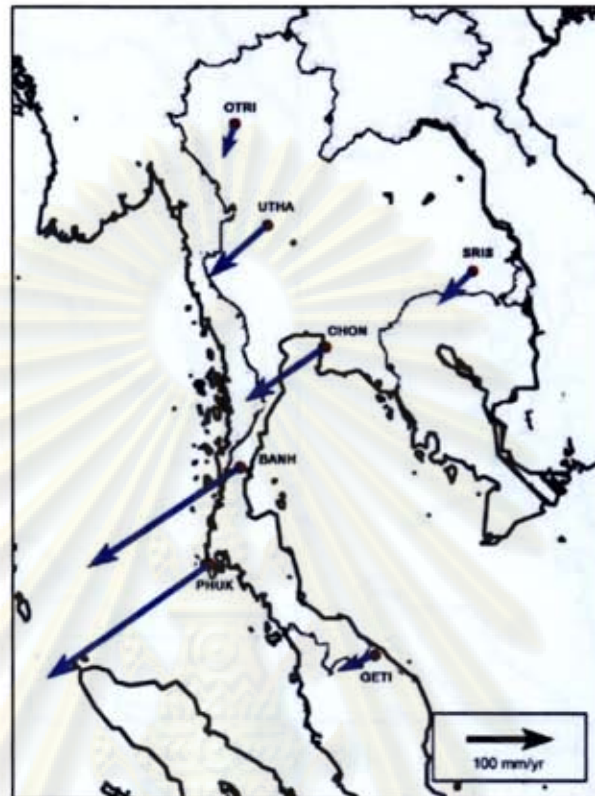
Figure 4.5 Velocity vectors of GPS sites at one and a half month after the Boxing-day
mega-earthquake.

4.2.3 After the Nias earthquake (between 28 Mar.2005 and 6 Nov. 2006)

After Nias Earthquake, it was found that all GPS stations illustrated a similar
effect as after the Boxing-day mega-earthquake. The velocity vectors were retaining the
same direction with only the reducing magnitude i.e. slower movement as time passed
(Figure 4.6)
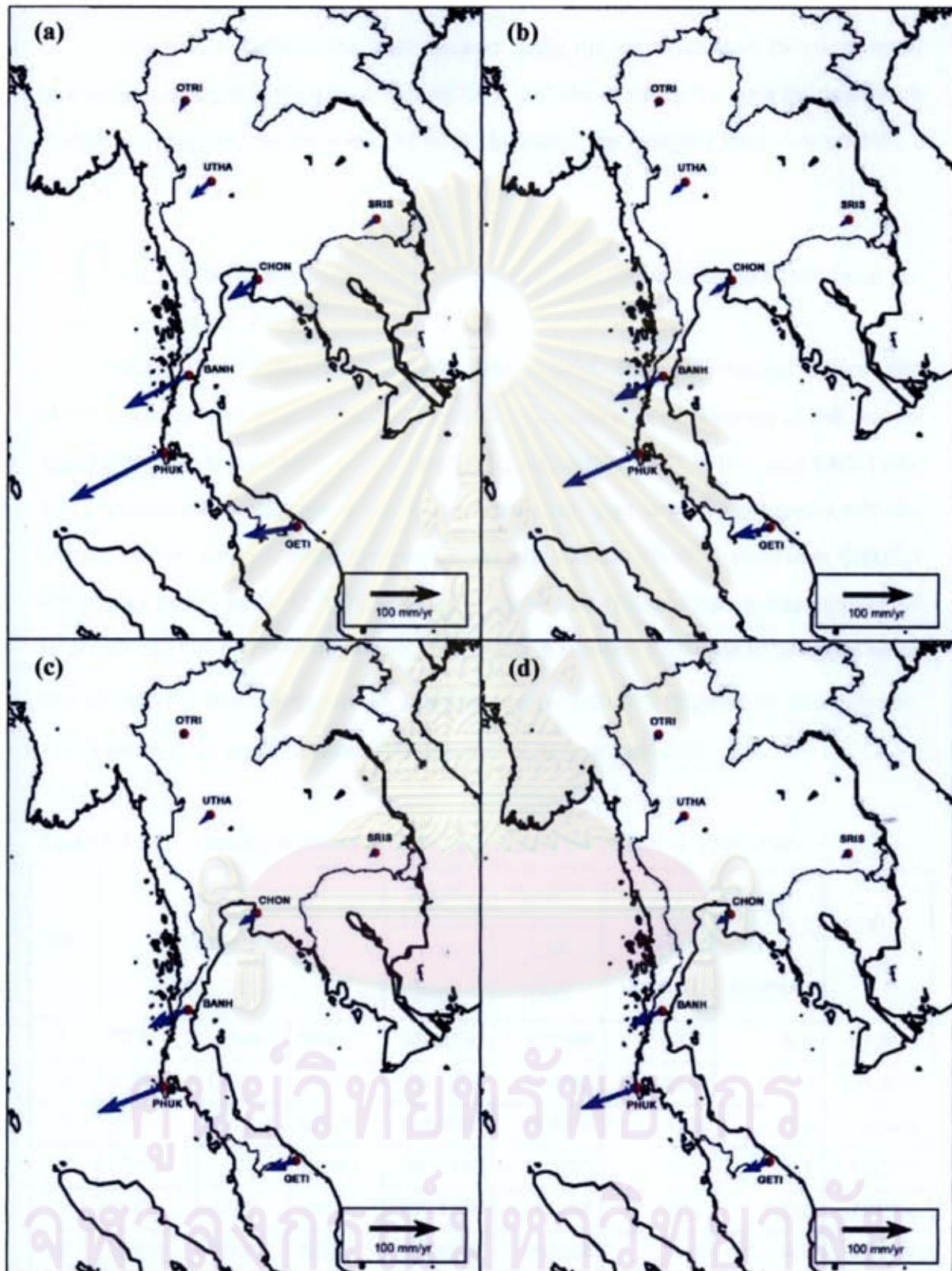
Figure 4.6 Velocity vectors of GPS sites at (a) 3 months, (b) 6 months, (c) 9 months and
(d) one year after the Nias earthquake

4.3 Strain Rate Tensors

The crustal deformation was studied using the representative principal strain rate within a triangle forming by 3 nearest GPS stations, in which the area inside of each triangle is assumed to be homogeneous. Similarly, the analysis was divided into 3 periods.

    4.3.1   Before the Boxing-day mega-earthquake (between 27 Nov. 1994 and 25 Dec. 2004)

During the 10-year period, from 1994 – 2004, Thailand's crustal deformation patterns varied from place to place. Principal strain rate was significantly of extensional type in Triangle 2 (see Table 4.1) in the west, marked by ORTI, UTHA and BANH site. The magnitude is a little less than 30 nanostraude per year which was agreed with the research work done by Iwakuni et al. (2004) which using the GPS data from GAME-T Project between 1998 and 2001 which also found that Thailand had a maximum shear strain around 10 – 40 nanostrain per year. Table 4.1 shows the value of principal strain rate ($\dot{\varepsilon}_1$ and $\dot{\varepsilon}_2$) which will consider positive as extension and negative as compression, and θ which is an angle between the direction of $\dot{\varepsilon}_2$ and the North.

Table 4.1   Results of principal strain rate during the period of 1994-2004

No.	Triangle Network			Position of Centroid		$\dot{\varepsilon}_1$ (nano strain/yr)	$\dot{\varepsilon}_2$ (nano strain/yr)	θ (deg)
				LON (deg)	LAT (deg)			
1	OTRI	UTHA	SRIS	101.2790	16.2185	7.5	-5.9	61.2627
2	OTRI	UTHA	BANH	99.4847	14.7766	25.9	-7.5	28.2457
3	UTHA	SRIS	CHON	101.8240	14.4763	-1.3	-3.4	-9.6526
4	UTHA	CHON	BANH	100.0418	13.0395	-3.2	-9.1	72.6971
5	CHON	SRIS	BANH	101.4974	12.8864	10.0	-8.2	24.2115
6	BANH	PHUK	GETI	99.8330	8.2014	1.2	-4.7	42.8725
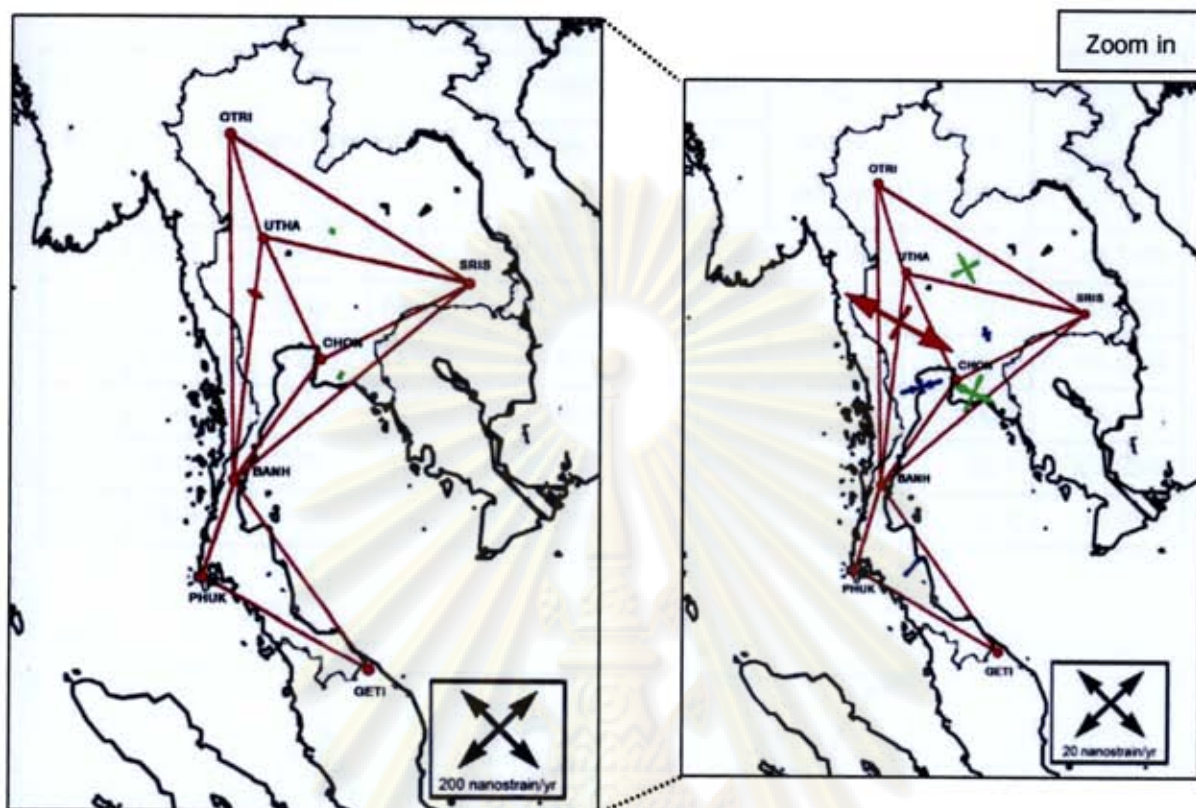
Figure 4.7 Strain rate tensors during 1994-2004. Red crossed arrow denote as extension significance. Blue crossed arrow denote as compression significance. Green crossed arrow denote as strike-slip significance.

4.3.2 After the Boxing-day mega-earthquake (26 Dec. 2004 – 28 Mar. 2005)

The crustal deformation was recalculated one and a half months after the Boxing-day mega-earthquake. It was found that crustal deformation pattern in Thailand had changes throughout the country by showing the principal strain rate as the extensional type in the Northeast – Southwest direction at the magnitude of approximately 0.3 microstrain per year (see Table 4.2). There are some notices that the direction of the principal strain rate to the southern area (Triangles 5 and 6) was slightly different from that in the upper part of country.

38

Table 4.2 Results of principal strain rate at one and a half months after the Boxing-day mega-earthquake

No.	Triangle Network			Position of Centroid		$\dot{\varepsilon}_1$	$\dot{\varepsilon}_2$	θ
				LON (deg)	LAT (deg)	(nano strain/yr)	(nano strain/yr)	(deg)
1	OTRI	UTHA	SRIS	101.2790	16.2185	202	-38.9	-45.7263
2	OTRI	UTHA	BANH	99.4847	14.7766	244	-40.0	-43.0952
3	UTHA	SRIS	CHON	101.8240	14.4763	155	-43.6	-39.5639
4	UTHA	CHON	BANH	100.0418	13.0395	290	-50.1	-38.3504
5	CHON	SRIS	BANH	101.4974	12.8864	299	-80.1	-67.9045
6	BANH	PHUK	GETI	99.8330	8.2014	372	-50.4	-16.3841

Figure 4.8 Strain rate tensors at one and a half month after the Boxing-day mega-earthquake

4.3.3   After the Nias earthquake (between 28 Mar.2005 and 6 Nov. 2006)

The strain after the Nias earthquake also retained the same characteristics with the period of one month after the earthquake. However, the magnitudes of principal strain rate tensors were smaller (see Table4.3). When the time passed by the magnitude become smaller. The direction angle of the principal strain in the southern area, Triangle 6, gradually changed course to be more parallel to the western part of country. (See Figure 4.9 and Table 4.4, 4.5 and 4.6)

Table 4.3   Results of principal strain rate at three months after the Nias earthquake

No.	Triangle Network			Position of Centroid		$\dot{\varepsilon_1}$ (nano strain/yr)	$\dot{\varepsilon_2}$ (nano strain/yr)	θ (deg)
				LON (deg)	LAT (deg)			
1	OTRI	UTHA	SRIS	101.2790	16.2185	92.9	-14.5	-47.5314
2	OTRI	UTHA	BANH	99.4847	14.7766	166	14.6	-24.8731
3	UTHA	SRIS	CHON	101.8240	14.4763	79.1	-18.6	-42.9051
4	UTHA	CHON	BANH	100.0418	13.0395	158	-11.3	-31.6358
5	CHON	SRIS	BANH	101.4974	12.8864	141	-132	-58.6056
6	BANH	PHUK	GETI	99.8330	8.2014	252	-36.0	-28.4160

Table 4.4   Results of Principal Strain rate at six months after the Nias earthquake

No.	Triangle Network			Position of Centroid		$\dot{\varepsilon_1}$ (nano strain/yr)	$\dot{\varepsilon_2}$ (nano strain/yr)	θ (deg)
				LON (deg)	LAT (deg)			
1	OTRI	UTHA	SRIS	101.2790	16.2185	67.7	-9.93	-47.8462
2	OTRI	UTHA	BANH	99.4847	14.7766	136	13.6	-21.6320
3	UTHA	SRIS	CHON	101.8240	14.4763	59.1	-13.4	-43.4435
4	UTHA	CHON	BANH	100.0418	13.0395	122	-6.85	-30.1767
5	CHON	SRIS	BANH	101.4974	12.8864	106	-114	-57.7009
6	BANH	PHUK	GETI	99.8330	8.2014	212	-23.4	-25.2392

Table 4.5   Results of principal strain rate at nine months after the Nias earthquake

No.	Triangle Network			Position of Centroid		$\dot{\varepsilon_1}$ (nano strain/yr)	$\dot{\varepsilon_2}$ (nano strain/yr)	θ (deg)
				LON (deg)	LAT (deg)			
1	OTRI	UTHA	SRIS	101.2790	16.2185	53.2	-7.49	-48.0249
2	OTRI	UTHA	BANH	99.4847	14.7766	114	11.8	-19.9715
3	UTHA	SRIS	CHON	101.8240	14.4763	47.1	-10.5	-43.7360
4	UTHA	CHON	BANH	100.0418	13.0395	99.3	-4.80	-29.3497
5	CHON	SRIS	BANH	101.4974	12.8864	85.3	-98.6	-57.2827
6	BANH	PHUK	GETI	99.8330	8.2014	183	-16.2	-23.4239

Table 4.6   Results of principal strain rate at a year after the Nias earthquake

| No.	Triangle Network			Position of Centroid		$\dot{\varepsilon_1}$ (nano strain/yr)	$\dot{\varepsilon_2}$ (nano strain/yr)	θ (deg)
				LON (deg)	LAT (deg)			
1	OTRI	UTHA	SRIS	101.2790	16.2185	43.8	-5.99	-48.1394
2	OTRI	UTHA	BANH	99.4847	14.7766	98.4	10.2	-18.9709
3	UTHA	SRIS	CHON	101.8240	14.4763	39.2	-8.62	-43.9189
4	UTHA	CHON	BANH	100.0418	13.0395	83.8	-3.66	-28.8181
5	CHON	SRIS	BANH	101.4974	12.8864	71.3	-86.1	-57.0453
6	BANH	PHUK	GETI	99.8330	8.2014	160	-11.3	-22.1777
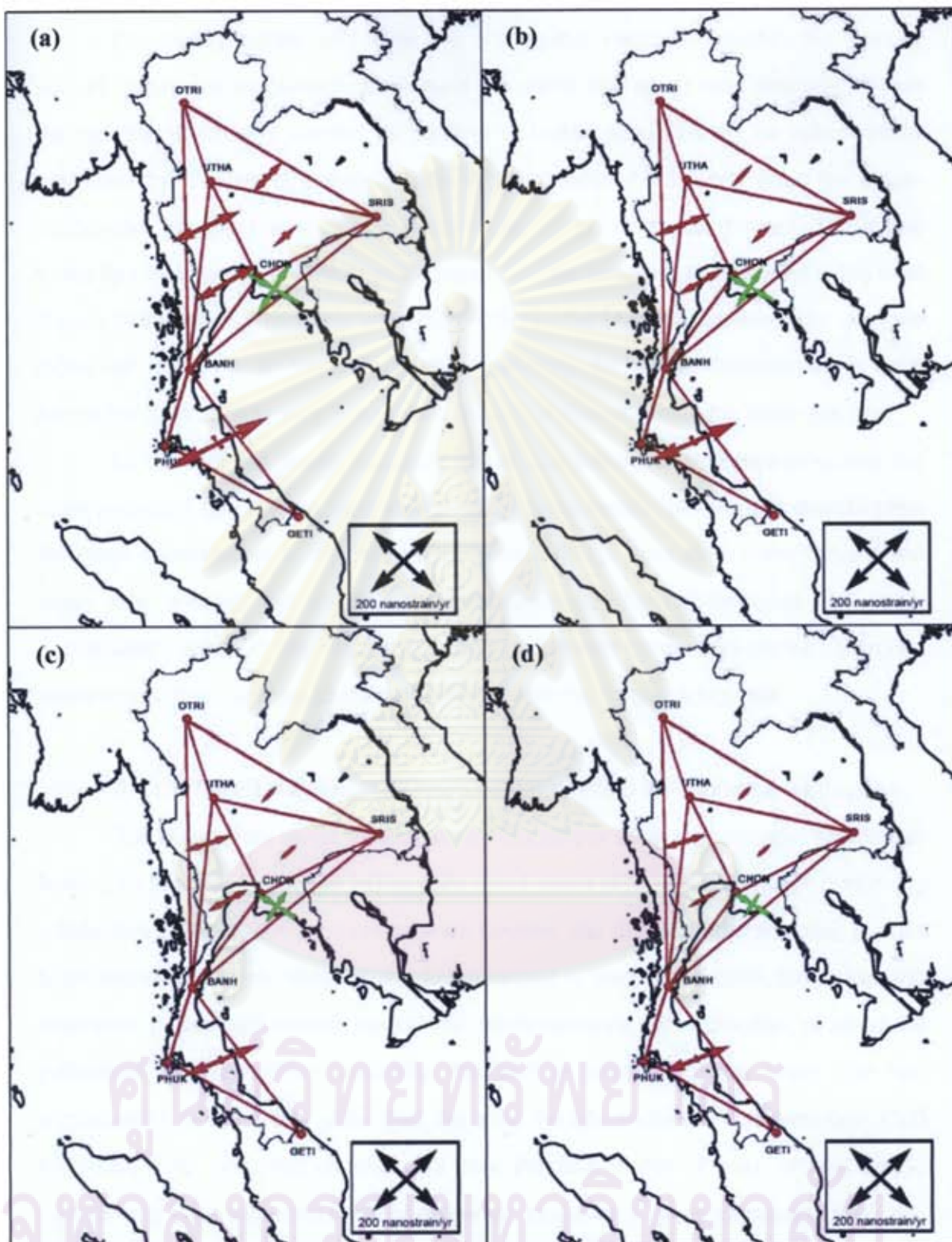
Figure 4.9 Strain rate tensors (a) 3 months, (b) 6 months, (c) 9 months and (d) one year after the Nias earthquake

4.4 Discussion

Comparing before and after the Boxing-day mega-earthquake, the velocity vectors before the mega-earthquake have the same east-south east direction all over the country, which was caused by pushing of Indian plate that will be subsequently explained by the lateral escape model in the Section 4.4.3, while after the mega-earthquake, the direction of velocity vectors was changed to the south-west. This is due to the fact that Myanmar platelet at the region around epicenter had slipped to the west toward Indian plate. Then, the crust connected to the Myanmar platelet was dragged along with. However, as the crust is not a rigid body, the rate of displacement in each part of the crust is different in magnitude, the nearer the epicenter, the faster the rate.

In case of the strain analysis, before the Boxing-day mega-earthquake the observed strain rate tensors were very small (< 30 nanostrain per year). It depicted that the block moved as an approximate rigid block although there were some value of the strain rate showed the crust was inhomogeneous. Nevertheless, as the strain accumulation released, the mega-earthquake occurrence caused the greater strain rate tensors more than 10 times of the magnitude before the mega-earthquake.

4.4.1 The 2004 Boxing-day mega-earthquake and the 2005 Nias earthquake

The Boxing-day mega-earthquake 26 December 2004 is associated with thrust-faulting on the interface of that Indian plate and Eurasia plate which has been continuing subduction process, oblique convergence involves slip directed approximately parallel to the Sumatran trench. With respect to the interior of the Eurasia plate, the Indian and Australian plates had moved toward the north-northeast with velocities of about 30 millimeters per year. Then suddenly, the faulting released elastic strain that had accumulated for centuries. After that, the zone the aftershocks, which were over 1300 kilometers long, occurred on and very near the fault planes of main shocks whose rupture may have extended north of epicenter. However, a great earthquake may also trigger earthquake activity on faults that are distinct from the main-shock fault plane and separated from it by tens or even hundreds of kilometers. (USGS, February 2005)
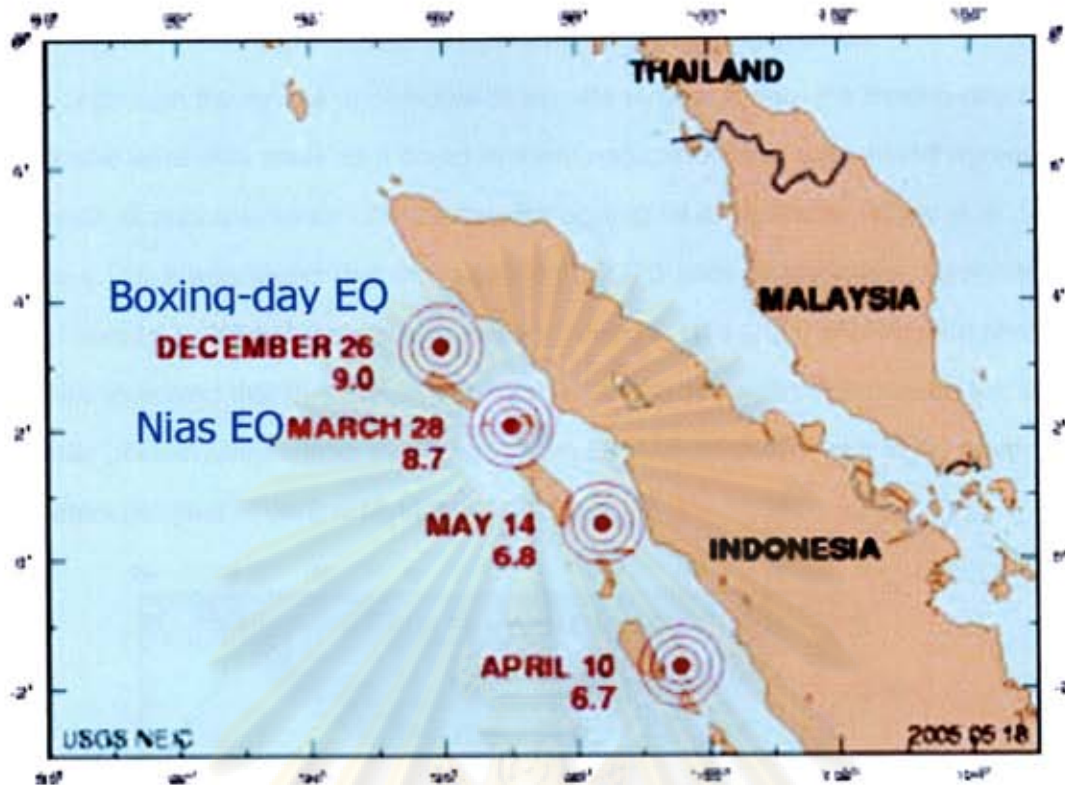
Figure 4.10 Epicenter of the Boxing-day mega-earthquake and the Nias
earthquake (USGS, May 2005)

Subsequently not so long, the Nias earthquake 28 March 2005 also occurred as oblique convergence, which is partitioned into thrust-faulting on the interface of the Australia plate and Eurasia plate. As the Australia plate subducts beneath the overriding Sunda plate, the Australia plate moves at a rate of about 5 cm/year toward the northeast relative to the Sunda plate and the stresses which caused the earthquake were developed at the Sunda trench. This earthquake was likely triggered by stress changes caused by the 26 December 2004 (M9.0) earthquake but it occurred on a segment of the fault 100 miles (160 kilometers) to the southeast of the main rupture zone. (USGS, April 2005)

In this research, it was found that the results of both earthquakes had shown a similar pattern by velocity vectors and principal strain rate tensors so it could indicate that the both earthquakes might had come from the same event, i.e., the Nias earthquake was a major aftershock of the Boxing-day mega-earthquake.

4.4.2 Crustal deformation in Myanmar and neighboring areas

Although the results of principal strain rate tensors before the Boxing-day mega-earthquake were very small as it could assume negligible. They were found agreed with the results of principal strain rate tensors at Sagaing fault, Myanmar (Vigny et al., 2003) (Figure 4.11). It was found that the velocities of GPS sites in Mandalay, Myanmar had moved about 10 – 40 millimeters per year northward in ITRF-2000 and western Myanmar velocities indicated that the total amount of right-lateral strike-slip deformation across the Myanmar platelet ranges from slightly less than 30 millimeters per year in the south to 25 millimeters per year in central Myanmar.
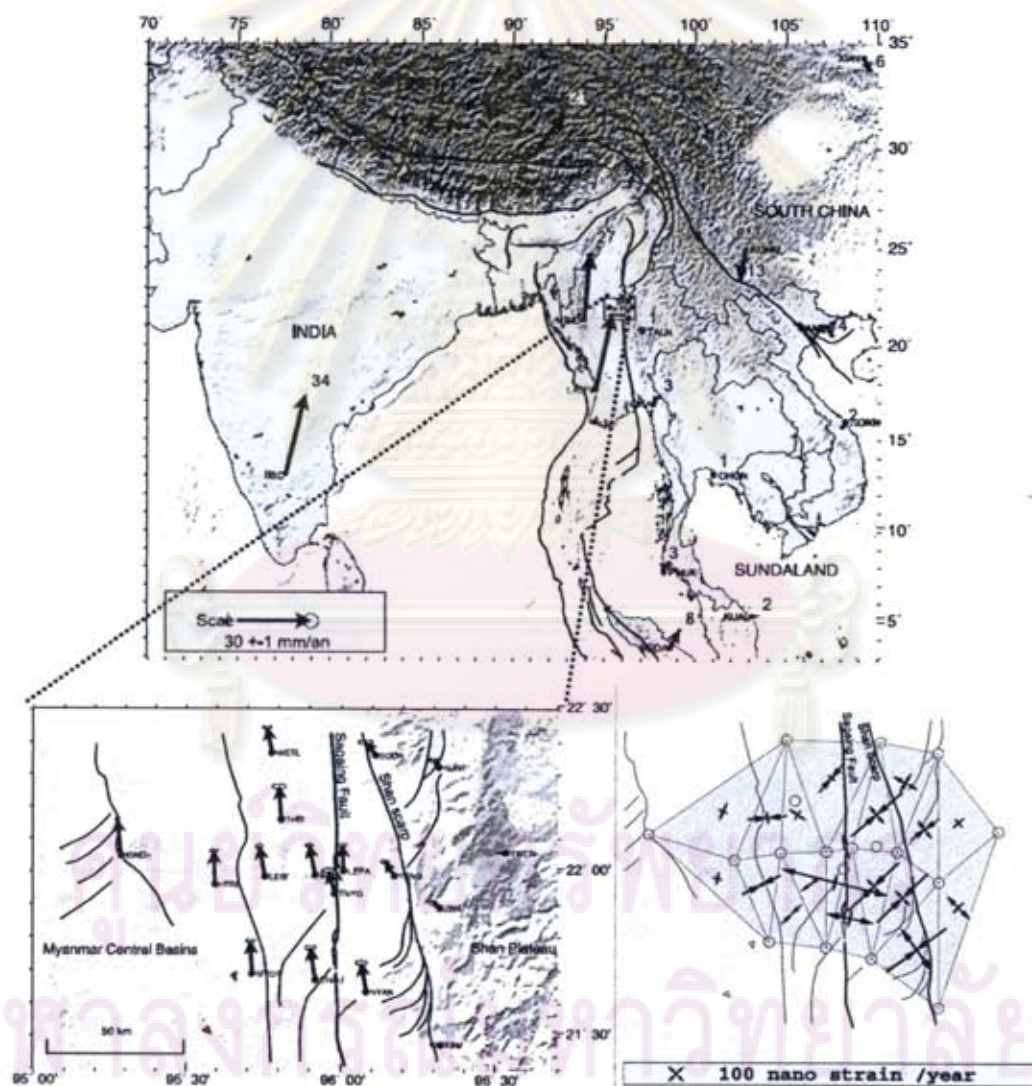

Figure 4.11 Regional and Myanmar velocities (top) with Mandalay area transect stations velocities (bottom left) and strain rates (bottom right) (modified after Vigny et al., 2003).

Comparing with the results of the principal strain rate tensors at Sagaing fault, the principal strain rate tensor of this study at the west in Figure 4.8 were almost the same direction as the direction of extensional type of the principal strain rate tensors at Sagaing fault.

4.4.3 The lateral escape

The work of Vigny et al. (2003) and this research may be further explained by the comment of Van der Pluijm and Marshak (2004). They mentioned that some of the movement on faults accommodates translation of large wedges of Asia relatively eastward, were in response to the collision of India with Asia. (Figure 4.12)
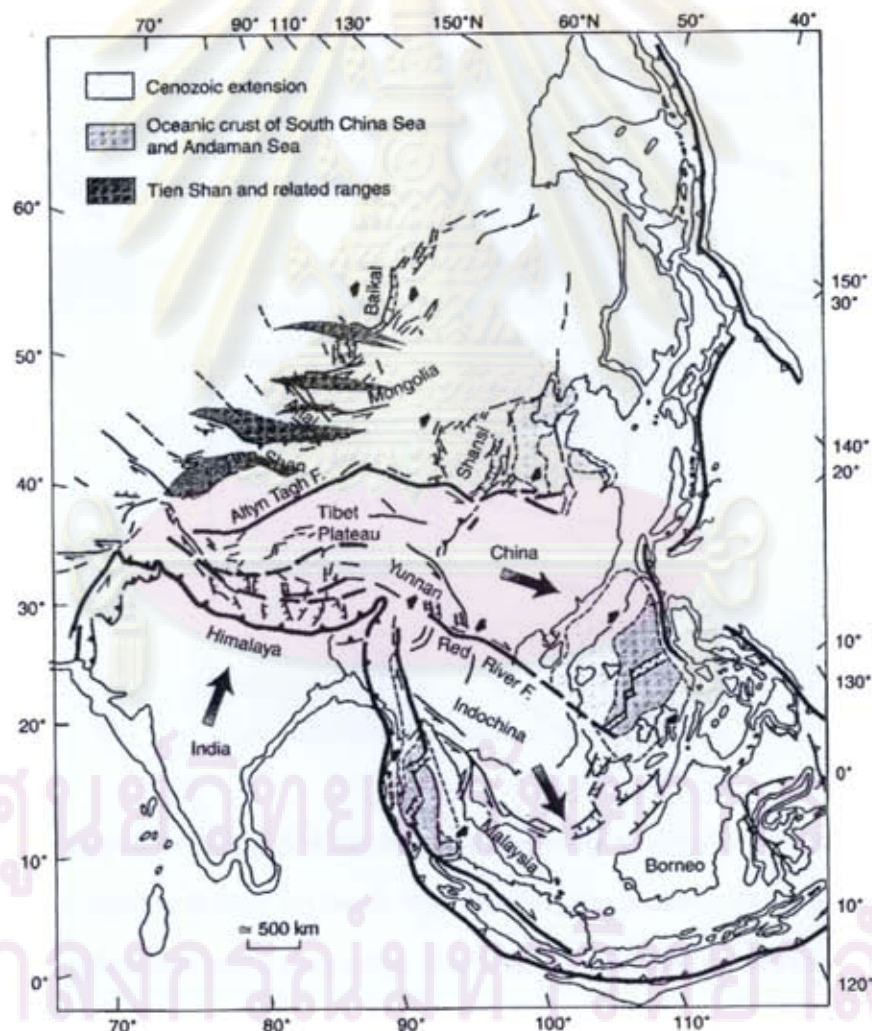
Figure 4.12   A sketch map of major structures in southeastern Asia. The large arrows indicate the motion of large crustal blocks (modified after Tapponnier et al., 1982 by Van der Pluijm and Marshak, 2004).

The simulation (Figure 4.13) showed the development of the faults by a model in which pushed a wooden block into a cake of clay. The wooden block represented the rigid craton of India, while the clay represented the relatively soft crust of Asia. In this model, a rigid wall, representing the mass of western Asia, constrained the left side of the clay cake. The right side, representing the Pacific margin, remained unconstrained. As the wooden block moved into the clay, wedges of clay, bounded by strike-slip faults, moved laterally to the right. The pattern of faults resembled the trajectories of maximum shear stress predicted by the theory of elasticity.
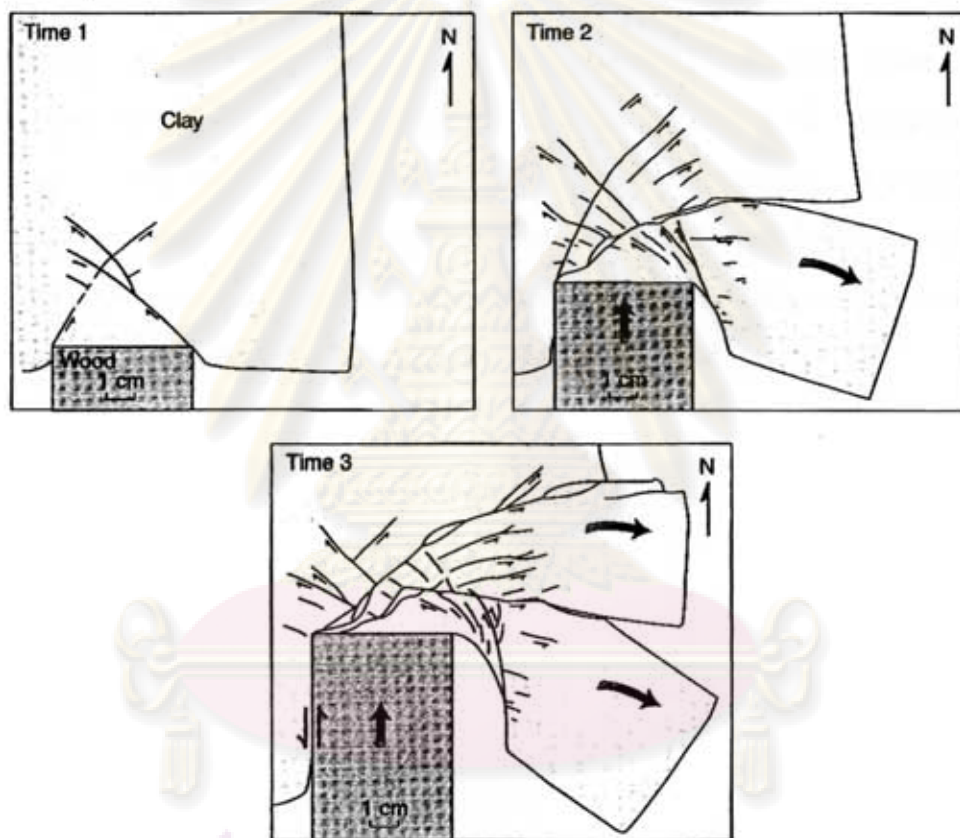
Figure 4.13   Map-view sketch of a laboratory experiment to simulate lateral-escape tectonics. A wooden block (representing the Indian craton) is pushed northwards into a clay cake. The cake is restrained on the west, but not on the east. As the block indents, strike-slip faults develop in the clay, and large slices are squeezed eastwards (modified after Tapponnier et al., 1982 by Van der Pluijm and Marshak, 2004).

4.4.4 Geotectonic of Thailand

Thailand is located in a part of the Sundaland block which consists of Vietnam, Laos, Cambodia, Thailand, Peninsular Malaysia, Sumatra, Borneo, Java and the shallow seas located in between (Sunda shelf). The rim of Sundaland block covers Sumatra and Java islands which are surrounded by 2 ocean plates, Indian Ocean plate and Pacific Ocean plate. Boundary of both ocean plates and Sundaland block is a continuous subduction zone which is caused by the collision between the Indian-Australian Plate and Eurasia Plate. Thailand consists of 2 major tectonic terranes, namely, Shan-Thai block and Indochina block (Bunopas and Vella, 1973, 1983). In addition, from the geological evidences, the Indian plate had moved toward Eurasia plate in the Cenozoic age making the compression in the line of North – South causing the right-lateral strike-slip faults in Thailand in the direction of Northwestern – Southeastern, i.e. Si Sawat Fault and Three Pagoda Fault which extended from North-South trending Sagaing fault in Myanmar (Charusiri et al., 2002), with the left-lateral displaced Northeastern – Southwestern, i.e. Ranong Fault and Khlong Marui Fault. (See Figure 4.14)

Figure 4.14 Active faults in Thailand (DMR, 2006)

Table 4.7 Summary of the active faults in Thailand and provinces that faults run across (after DMR, 2006)

Fault Name	List of Provinces
Mae Chan and Mae Ing	Chiang Rai and Chiang Mai
Mae Hong Son	Mae Hong Son and Tak
Mae Tha	Chiang Mai, Lamphun and Chiang Rai
Mae Yom	Phrae
Thoen	Lampang and Phrae
Moei	Tak and Kamphangphet
Phayao	Lampang, Chiang Rai and Phayao
Pua	Nan
Uttaradit	Uttaradit
Three Pagoda	Kanchanaburi and Ratchaburi
Si Sawat	Kanchanaburi and Uthai Thani
Tha Khaek	Nong Khai and Nakhon Phanom
Ranong	Prachuap Khiri Khan, Chumphon, Ranong and Phang Nga
Khlong Marui	Surat Thani, Krabi and Phang Nga

Table 4.7 shows the summary of the active faults in Thailand. These cover the 22 provinces of Mae Hong Son, Chiang Rai, Chiang Mai, Lamphun, Lampang, Phrae, Nan, Phayao, Tak, Kamphangphet, Uttaradit, Kanchanaburi, Ratchaburi, Uthai Thani, Nong Khai, Nakhon Phanom, Prachuap Khiri Khan, Chumphon, Ranong, Surat Thani, Krabi and Phang Nga. As the result of this research, these faults might have effects from the Boxing-day mega-earthquake which need to investigate more in the field.

4.4.5   Tectonic deformation from observing strain ellipsoids

Figure 4.15 illustrates the strain ellipsoids compared to the strain calculated from pre-mega earthquake. This confirms that their relationship has the same pattern as the movement of Sagaing fault in Myanmar which has been previously interpreted as being a plate boundary between India and Sundaland (Vigny et al., 2003).
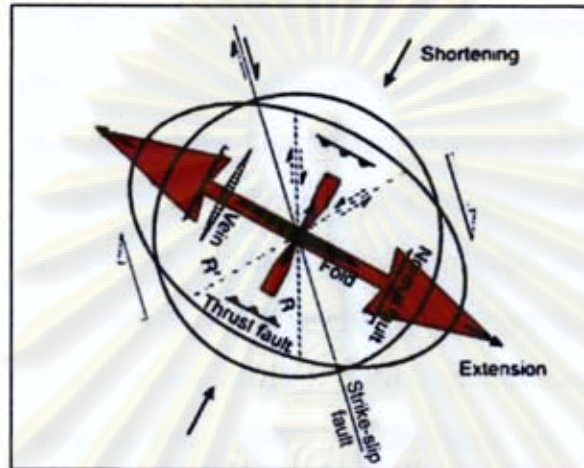
Figure 4.15 Strain ellipsoid compared with calculated strain rate tensor of triangle from the station of ORTI, UTHA and BANH (Triangle 2 in Figure 4.8)

Similarly, Figure 4.16 illustrates the strain ellipsoid compared with strain calculated from post-seismic, it was found that this Megathrust earthquake has also been sliding as right-lateral oblique faulting which is agreeable with movement of Sumatran trench, as explained in Section 4.4.2.
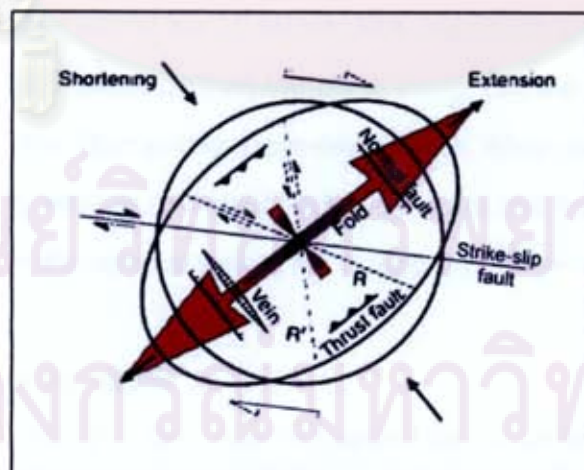
Figure 4.16 Strain ellipsoid compared with calculated strain rate tensor of a particular triangle in Figure 4.9

CHAPTER V
CONCLUSION AND RECOMMENDATION FOR FURTHER STUDY

5.1 Conclusion

Thailand is a part of Sundaland block which is considered as a rigid plate (Chamot-Rooke and Le Pichon, 1999); however, after the mega-earthquake incident on the December 26, 2004, there was an effect all over the region near the epicenter which was close to Banda Aceh, Indonesia. This research have studied on Thailand movement by processing the GPS data from 6 regional GPS sites consisting of Phuket, Chumporn, Chonburi, Uthaithanee, Srisaket and Lampang in Thailand, and the GPS data from a station located in the northern part of Malaysia for both periods of before and after the Boxing-day mega-earthquake. It was found that about 10 years before the Boxing-day mega-earthquake, Thailand had moved to the east with the average rate of approximately 33.2 ± 1.1 millimeters per year and had less than 30 nano-strain per year horizontal strain rate tensors. Northwestern part, which is the standout part on the time, showed the same pattern as the movement of Sagaing fault, Myanmar. After the Boxing-day mega-earthquake, Thailand had horizontal movement in the southwest direction at the different rates in each part, higher velocity from the north to the south. The horizontal strain rate tensors were the extension type in the direction of northeast – southwest all over country agreed with the movement of Sumatran trench. In addition, these kinds of results is also resemble with of the 28 March 2005 Nias earthquake so it could indicate that both Earthquakes may come from the same event, i.e., the Nias earthquake was a major aftershock of the Boxing-day mega-earthquake. When the time passed by, the magnitude of velocity vectors and strain rate tensors are smaller so later, the pattern of deformation might be the same as before the Boxing-day mega-earthquake occurred.

5.2 Recommendation for Further Study

As there are not many GPS sites in Thailand that make them far from each other, the results of the study just a coverage of the country area but it could not see in details in some small areas that there may be some different deformations in some local areas. Moreover, the size of triangle was quite large and strain was probably concentrated in a

very small part of it so it cannot be indicated where the exact change should be. However, a large GPS network for study about earth's deformation may not yet appropriate for Thailand because it does not have a lot of change in short time but study only small area such as a fault is needed to investigate whether it is active is possible to do by using GPS campaign.

As strain is defined as the shape change and strain analysis attempts to quantify the magnitude and/or the orientation of the strain ellipsoids in rocks and regions using the development of mathematical tool, a common goal in strain analysis is to compare results obtained in one place with those obtained in another place. Strain rate is a long-term study that needs continuous observations. As strain accumulation is a long-term change that may accumulate energy until reaching the rupture points of the materials, so at the weak point such as a fault may cause earthquake. Relationships and statistics should be studied in correlation with other field study such as seismology, paleontology, etc. to understand the phenomena in various dimensions. For example, relationships between geologic structures and geodetic observations of regional tectonic strain can be correlated with potential geothermal resources (Blewitt et al., 2003). Studies with statistics upon the geological evidences, such as fossil, can obtain the history data of strain accumulation, which may compare with the strain accumulation obtained from GPS measurement. These may give a better understanding about the change from the past to the present.

Furthermore, strain rate is one of fundamental parameters which is used to describe the ability of stressed material to deform or to flow so called "Rheology". The ultimate goal to study strain or deformation of the Earth's crust is to understand the phenomena of earthquakes, which may help to the prediction of earthquakes.

REFERENCES

Blewitt, G., Coolbaugh, M., Sawatzky, D., Holt, W., Davis, J. and Bennett, R. Targeting of Potential Geothermal Resources in the Great Basin from Regional to Basin-Scale Relationships between Geodetic Strain and Geological Structures. Transactions Geothermal Resources Council, GRC Meeting. Morelia, Mexico, October 2003.

Beutler, G., Mueller, I. I. and Neilan, R. E. The International GPS Service for Geodynamics (IGS): Development and start of official service on January 1, 1994. Bulletin Geodesique, 68 (1994): 39–70.

Bunopas, S. and Vella, P. Late Paleozoic and Mesozoic Structural evolution of northern Thailand – a plate tectonic model. Proceeding of the Third Regional Conference on Geolory and Mineral Resources of Southeast Asia, III GEOSEA, pp.133-140. Bangkok, 1978.

Bunopas, S. and Vella, P. Tectonic and geologic evolution of Thailand: Proceeding of the workshop on stratigraphic correlation of Thailand and Malaysia. Journal of the Geological Society of Thailand, 1 (1983): 307-318.

Chamot-Rooke, N., and Le Pichon, X. GPS determined eastward Sundaland motion with respect to Eurasia confirmed by earthquakes slip vectors at Sunda and Philippine trenches. Earth and Planetary Science Letter 173 (1999): 439-455.

Charusiri, P., Daorerk V., Archibald, D., Hisada, K. and Ampaiwan, T. Geotectonic evolution of Thailand: A new synthesis. Journal of the Geological Society of Thailand, 1 (2002): 1-20.

Cai, J. and Grafarend, E. Statistical analysis of geodetic deformation (strain rate) derived from the space geodetic measurements of BIFROST Project in Fennoscandia. Journal of Geodynamics, 43 (2007): 214-238.

Condie, K. C. Earth as an evolving planetary system. London: Elsevier Academic Press, 2005.

Dana, P.H. Global Positioning System Overview [Online]. 2000. Available from: http://www.colorado.edu/geography/gcraft/notes/gps/gps_f.html

Department of Mineral Resources [DMR]. Active fault zones in Thailand [Online]. 2006. Available from: http://www.dmr.go.th/

El-Rabbany, A. Introduction to GPS: the global positioning system. Massachussets: Artech House, 2002.

Hashimoto, M., Choosakul, N., Hashizume, M., Takemoto, S., Takiguchi, H., Fukuda, Y., and Fujimori, K. Crustal deformations associated with the great Sumatra-Andaman earthquake deduced from continuous GPS observation. Earth Planets Space 58 (2006): 127-139.

Hibberaler, R.C. Mechanics of Materials. 3rd ed. New Jersey: Prentice Hall, 1997.

Integrated Ocean Drilling Program [IODP]. Proceedings of the Ocean Drilling Program, Initial Reports Volume 193 [Online]. 2002. Available from: http://www-odp.tamu.edu/publications/193_IR/chap_02/c2_f12.htm

Iwakuni, M. Tectonics in east Asia as seen from GPS data. Doctoral dissertation, Department of Earth and Planetary Science, Graduate School of Science, University of Tokyo, 2006.

Iwakuni, M., Kato, T., Takiguchi, H., Nakaegawa, T., and Satomura, M. Crustal deformation in Thailand and tectonics of Indochina peninsula as seen from GPS observations. Geophysical Research Letters 31 (2004): L11612.

Jordan, M. A. The Balcones fault zone of Austin [Online]. (n.d.). Available from: http://www.lib.utexas.edu/geo/ggtc/ch3.html [2006, July 24]

Kobayashi, T. and Hashimoto, M. Change of strain rate and seismicity in the Chubu district, central Japan, associated with a Tokai slow event. Earth Planets Space. 59 (2007): 351-361.

Kreemer, C., Haines, J., Holt, W. E., Blewitt, G., and Lavallee, D. On the determination of a global strain rate model. Earth Planets Space. 52 (2000): 765-770.

Marone, C., Scholz, C. H. and Bilham, R. On the mechanics of earthquake afterslip, Journal Geophysical Research, 96 (1991): 8441-8452.

McInerney, P., Guillen, A., Courrioux, G., Calcagno, P. and Lees, T. Building 3D Geological Models Directly from the Data? A New Approach Applied to Broken Hill, Australia. Digital Mapping Techniques '05—Workshop Proceedings. [Online]. 2005. Available from: http://pubs.usgs.gov/of/2005/1428/mcinerney/ index.html

Means, W. D. Stress and strain: basic concepts of continuum mechanics for geologists. New York: Springer-Verlag, 1976.

Michel, G. W., Becker, M., Angermann, D., Reigber, C., and Reinhart, E. Crustal motion in E- and SE-Asia from GPS measurements. Earth Planets Space 52 (2000): 713-720.

Michel, G. W., Yu, Y. Q., Zhu, S. Y., Reigber, C., Becker, M., Reinhart, E., Simons, W., Ambrosius, B., Vigny, C., Chamot-Rooke, N., Pichon, X. L., Morgan, P., and Matheussen, S. Crustal motion and block behavior in SE-Asia from GPS measurements. Earth and Planetary Science Letters 187 (2001): 239-244.

Pidwirny, M. Fundamentals of Physical Geography [Online]. 2nd ed. (E-book), 2006. Available from: http://www.physicalgeography.net/fundamentals/contents.html

Ritter, M. E. The Physical Environment: an Introduction to Physical Geography [Online]. 2006. Available from: http://www.uwsp.edu/geo/faculty/ritter/geog101/textbook/title_page.html

Ryan, S. Cliffsquickreview earth science. New Jersey: Wiley Publishing, 2006.

Satirapod, C. Improving the GPS Data Processing Algorithm for Precise Static Relative Positioning. Doctoral dissertation, School of Surveying and Spatial Information Systems, The University of New South Wales, 2002

Satirapod, C., Laoniyomthai, N. and Chabangborn, A. Crustal Movement of Thailand Disc Due to the 28 March 2005 earthquake as observed from GPS measurements. International Journal of Geoinformatic 3(1) (2007): 29-33.

Satirapod, C., Simons, W., Promthong, C., Yousamran, S. and Trisirisatayawong, I. Deformation of Thailand as detected by GPS measurements due to the December 26th, 2004 mega-thrust Earthquake. Survey Review 39(304) (2007): 109-115.

Satirapod, C., Simons, W. J. F. and Promthong, C. Monitoring deformation of Thai geodetic network due to the 2004 Sumatra-Andaman and 2005 Nias earthquake by GPS. Journal of Surveying Engineering. 134(3) (August 2008): 83-88.

Simons, W. J. F., Ambrosius, B. A. C., Noomen, R., Angermann, D., Wilson, P., Becker, M., Reinhart, E., Walpersdorf, A. and Vigny, C. Observing Plate Motions in S.E. Asia: Geodetic Results of the GEODYSSEA Project. Geophysical Research Letters, 26(14) (1999), 2081–2084.

Simons, W. J. F., Ambrosius, B.A.C., Yousamran, S. and Promthong, C. Deformation of Thailand measured by GPS due to the December 2004 mega-thrust earthquake. DEOS official report to RTSD. pp. 14. Delft, The Netherlands, 2005.

Simons, W.J.F., Socquet, A., Vigny, C., Ambrosius, B.A.C., Matheussen, S., Haji Abu, S., Subarya, C., Sarsito, D.A., Promthong, C., Iwakuni, M., Morgan, P., and Spakmen, W. A decade of GPS measurements in Southeast Asia: Resolving Sundaland motion and boundaries. Journal of Geophysical Research 112 (2007): B06420.

Shen, Z., Jackson, D. and Kagan, Y. Implications of geodetic strain rate for future earthquakes, with a five-year forecast of M5 earthquakes in Southern California. Seismological Research Letters. 78(1) (2007):116-120.

Socquet, A., Vigny, C., Chamot-Rooke, N., Simons, W. J. F., Rangin, C. and Ambrosius, B. India and Sunda plates motion and deformation along their boundary in Myanmar determined by GPS. Journal of Geophysical Research. 111 (2006): B05406.

Tapponnier, P., Peltzer, G., Le Bain, A. Y., Armijo, R. and Cobbold, P. Propagating extrusion tectonics in Asia: new insight from simple experiments with plasticine. Geology, 10 (1982): 611-616. Cited in Van der Pluijm, B.A. and Marshak, S. Earth structure: an introduction to structure geology and tectonics. 2nd ed. New York: W. W. Norton & Company, 2004.

Turcotte, D.L. and Gerald, S. Geodynamics. 2nd ed. New York: Cambridge University Press, 2002.

Terada, T., and Miyabe, N. Deformation of earth crust in Kiransai District and its relation to the orographic feature. Bull. Earth Res. Inst. 7 (1929): 223–241. Cited in Cai, J. and Grafarend, E. Statistical analysis of geodetic deformation (strain rate) derived from the space geodetic measurements of BIFROST Project in Fennoscandia. Journal of Geodynamics 43 (2007): 214-238.

USGS. Earthquake poster summary [Online]. February 2005. Available from:
 http://earthquake.usgs.gov/eqcenter/eqarchives/poster/2004/20041226.php

USGS. Earthquake poster summary [Online]. April 2005. Available from:
 http://earthquake.usgs.gov/eqcenter/eqarchives/poster/2005/20050328.php

USGS. Magnitude 6.7 - NIAS REGION, INDONESIA – usybai [Online]. May 2005.
 Available from: http://earthquake.usgs.gov/eqcenter/eqinthenews/2005/usybai/

Van der Pluijm, B.A. and Marshak, S. Earth structure: an introduction to structure
 geology and tectonics. 2nd ed. New York: W. W. Norton & Company, 2004.

Vigny, C., Socquet, A., Rangin, C., Chamot-Rooke, N., Pubellier, M., Bouin, M., Bertrand,
 G., and Becker, M. Present-day crustal deformation around Sagaing fault,
 Myanmar. Journal of Geophysical Research 108 (2003): 2533.

Vigny, C., Simons, W., Abu, S., Ronnachai, B., Satirapod, C., Chhoosakul, M., Subarya,
 C., Omar, K., Abidin, H.Z., Socquet, A. and Ambrosius, B.A.C. Insight into the
 2004 Sumatra–Andaman earthquake from GPS measurements in southeast Asia.
 Nature 436 (2005): 201-206.

Ward, S. N. On the consistency of earthquake moment rates, geological fault data, and
 space geodetic strain: the United States. Geophysical Journal International. 134
 (1998): 172-186.

Wilson, P., Rais, J., Reigber, C., Reinhart, E., Ambrosius, B. A. C., Le Pichon, X., Kasser,
 M., Suharto, P., Majid, A., Awang, P., Almeda, R. and Boonphakdee, C. Study
 Provides Data on Active Plate Tectonics in Southeast Asia Region. Eos
 Transaction AGU, 79(45) (1998), 545.

ศูนย์วิทยทรัพยากร
จุฬาลงกรณ์มหาวิทยาลัย

APPENDICES

APPENDIX A: Value of Parameters

Table A-1 Coseismic and postseismic best-fit logarithmic model parameters for the two earthquakes (after Satirapod, 2008)

Station$_{Direction}$	Validity	a (cm)	τ_{log} (year)	c (cm)	R^2
BANH$_{North}$	12-26-04 to 11-06-06	-3.2	0.143	-7.5	0.9815
BANH$_{East}$	12-26-04 to 11-06-06	-7.5	0.291	-15.5	0.9970
CHON$_{North}$	12-26-04 to 11-06-06	-2.0	0.183	-3.8	0.9822
CHON$_{East}$	12-26-04 to 11-06-06	-2.9	0.177	-6.8	0.9977
ORTI$_{North}$	12-26-04 to 11-06-06	-0.9	0.095	-2.2	0.9761
ORTI$_{East}$	12-26-04 to 11-06-06	-0.7	0.399	-2.3	0.7726
PHUK$_{North1}$	12-26-04 to 03-28-05	-2.6	0.064	-10.1	0.9996
PHUK$_{East1}$	12-26-04 to 03-28-05	-2.5	0.006	-23.6	0.9996
PHUK$_{North2}$	03-28-05 to 11-06-06	-4.1	0.072	-9.5	0.9934
PHUK$_{East2}$	03-28-05 to 11-06-06	-15.7	0.624	-28.1	0.9983
SRIS$_{North}$	12-26-04 to 11-06-06	-0.7	0.062	-1.8	0.8480
SRIS$_{East}$	12-26-04 to 11-06-06	-1.1	0.154	-3.3	0.9757
UTHA$_{North}$	12-26-04 to 11-06-06	-1.7	0.151	-3.9	0.9860
UTHA$_{East}$	12-26-04 to 11-06-06	-2.0	0.166	-4.7	0.9738
GETI$_{North1}$	01-11-05 to 03-24-05	1.00E+03	525.4	-0.3	0.7854
GETI$_{East1}$	01-11-05 to 03-24-05	-0.5	0.002	-7.9	0.9241
GETI$_{North2}$	03-29-05 to 12-28-05	-577	407.1	-2.3	0.7436
GETI$_{East2}$	03-29-05 to 12-28-05	-6.0	0.284	-8.3	0.9709

APPENDIX B: Eigenvalue and Eigenvectors

Eigenvalues and eigenvectors are interesting for at least two reasons:

1. The can be used to provide solutions to coupled differential equations.

2. They have be used to find the directions of maximum variance.

Definition of Eigenvalue and Eigenvectors

Generically, an eigenvector of a matrix $\mathbf{A}$ is only scaled, not rotated, when operated on by $\mathbf{A}$.

$$\mathbf{A}x = \lambda x \qquad \text{(B-1)}$$

$$x \equiv \text{eigenvector}$$
$$\lambda \equiv \text{eigenvalue}$$

As means of finding the eigenpairs note that (B-1) can be written as

$$(\mathbf{A} - \lambda \mathbf{I})x = 0 \qquad \text{(B-2)}$$

The only way for (B-2) to have a non-trivial solution is for the tensor in the parenthesis to have zero determinant. Thus, the governing equation for the eigenvalues is given by

$$\det(\mathbf{A} - \lambda \mathbf{I})x = 0 \qquad \text{(B-3)}$$

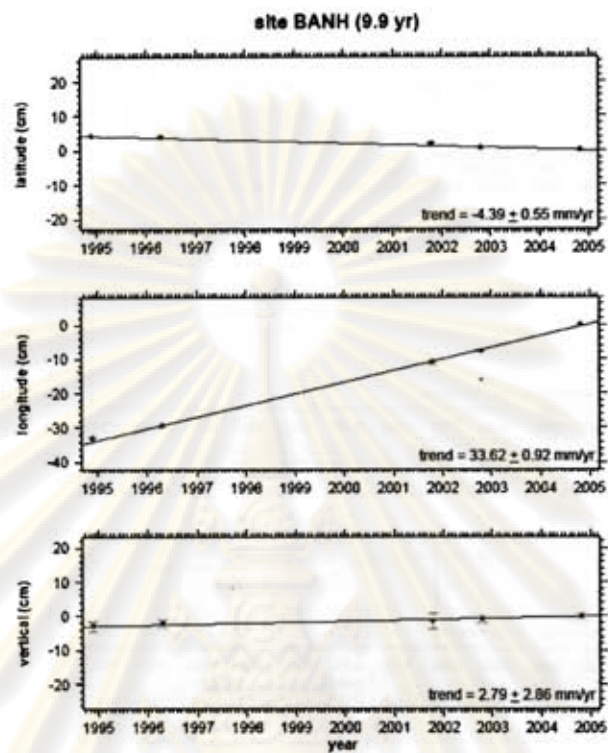APPENDIX C: Coordinate Time Series during 1994-2004 (Simon et al., 2007)

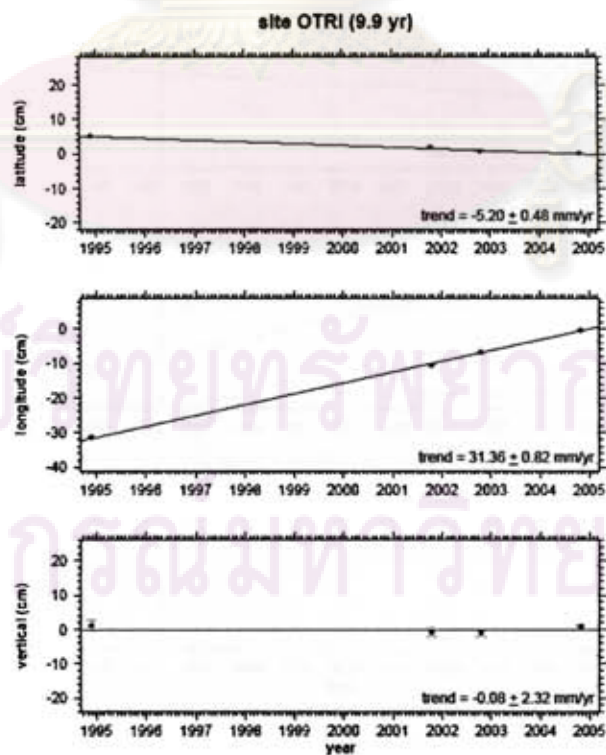Figure C-1 Coordinate Time Series of Chumporn (BANH) site

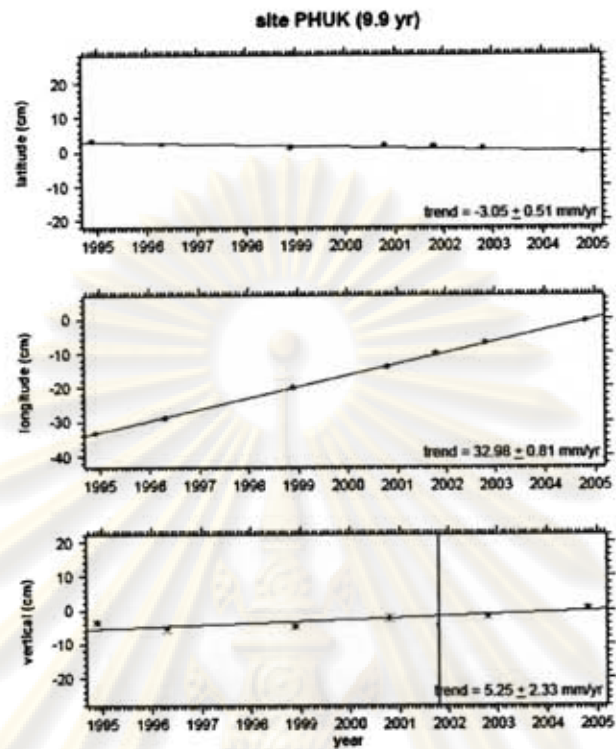Figure C-2 Coordinate Time Series of Lampang (ORTI) site

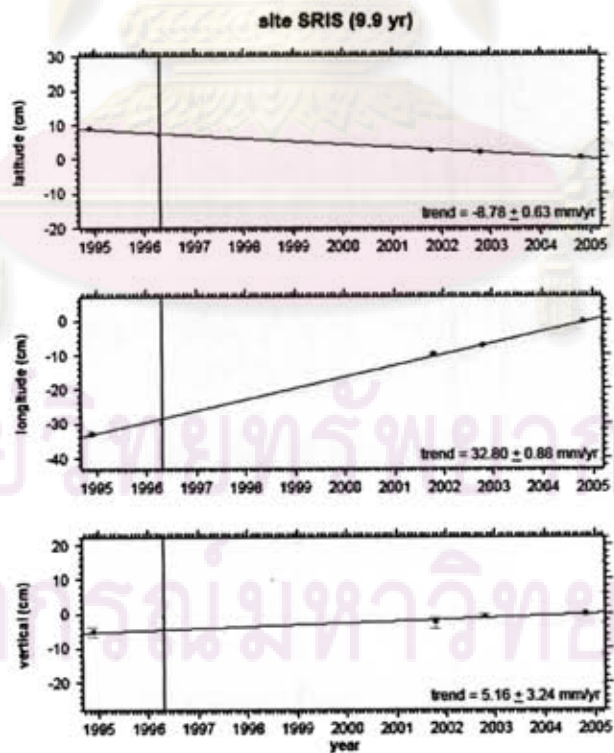Figure C-3 Coordinate Time Series of Phuket (PHUK) site

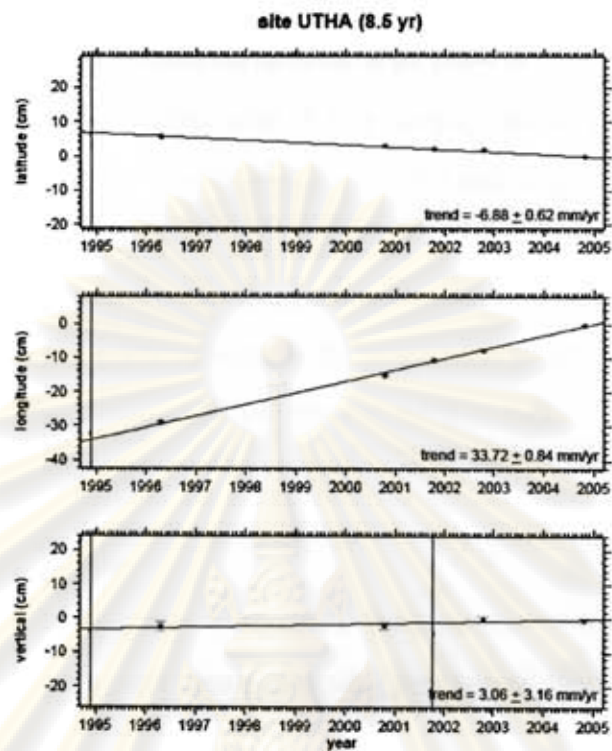Figure C-4 Coordinate Time Series of Srisaket (SRIS) site

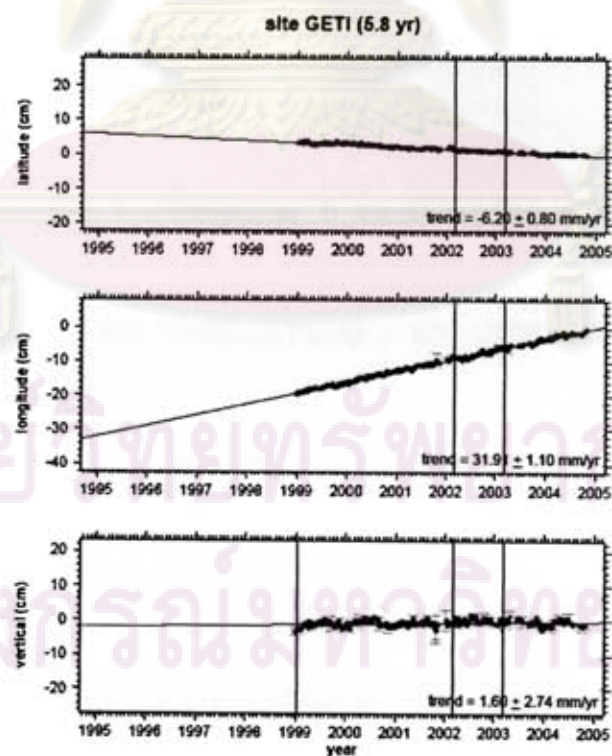Figure C-5 Coordinate Time Series of Uthaitani (UTHA) site

Figure C-6 Coordinate Time Series of Geting, Malaysia (GETI) site

CURRICULUM VITAE

Sarandhorn BAMRUNGWONG was born in Chiang Mai, Thailand, on March 24th, 1981. She received Bachelor of Engineering (Naval Architecture and Marine Engineering) in 2003 from Department of Mechanical Engineering, Faculty of Engineering, Chulalongkorn University. She worked as a volunteer for two years in a non-profit organization, International Buddhist Society. She started as a Master's student in Earth Sciences program, Department of Geology, Faculty of Science, Chulalongkorn University in 2005 and completed the program in October 2008.

Publication list

1. Conference presentation

    – Bamrungwong, S. Strain analysis in Thailand after the 26th December 2004 Earthquake using GPS measurements. The Annual Conference of GISTDA of year 2007. Bangkok, Nov. 28-30, 2007.

    – Bamrungwong, S. Change of strain rate in Thailand before and after the 26th December 2004 Earthquake using GPS measurements and preliminary geological interpretation. The Annual Conference of GISTDA of year 2008. Bangkok, Jan. 21-23, 2009.

2. Journal

    – Satirapod,C. and Bamrungwong, S. Strain analysis in Thailand after the 26th December 2004 Earthquake using GPS measurements. Journal of Remote Sensing and GIS Association of Thailand. 9(1) (2008): 1-6.